Journal of Environmental Management 342 (2023) 118307

Contents lists available at ScienceDirect

Journal of Environmental Management

journal homepage: www.elsevier.com/locate/jenvman

Review

Recent developments in metallic-nanoparticles-loaded biochars synthesis and use for phosphorus recovery from aqueous solutions. A critical review

Salah Jellali [a,*], Samar Hadroug [b], Malik Al-Wardy [c], Hamed Al-Nadabi [a], Najat Nassr [d], Mejdi Jeguirim [e,f]

[a] Centre for Environmental Studies and Research, Sultan Qaboos University, Al-Khoudh 123, Muscat, Oman
[b] Wastewaters and Environment Laboratory, Water Research and Technologies Centre, Carthage University, Soliman, 2050, Tunisia
[c] Department of Soils, Water and Agricultural Engineering, College of Agriculture and Marine Sciences, Sultan Qaboos University, Al-Khoudh 123, Muscat, Oman
[d] Rittmo Agroenvironnement, ZA Biopôle, 37 Rue de Herrlisheim, CS 80023, F-68025 Colmar Cedex, France
[e] Institut de Science des Matériaux de Mulhouse (IS2M), Université de Haute-Alsace, CNRS, UMR, 7361, F-68100, Mulhouse, France
[f] Institut de Science des Matériaux de Mulhouse (IS2M), Université de Strasbourg, CNRS, UMR, 7361, F-67081, Strasbourg, France

ARTICLE INFO

Handling Editor: Lixiao Zhang

Keywords:
Phosphorus
Wastewaters
Pristine biochars
Modified biochars
Recovery
Mechanisms

ABSTRACT

Phosphorus (P) represents a major pollutant of water resources and at the same time a vital element for human and plants. P recovery from wastewaters and its reuse is a necessity in order to compensate the current important depletion of P natural reserves. The use of biochars for P recovery from wastewaters and their subsequent valorization in agriculture, instead of synthetic industrial fertilizers, promotes circular economy and sustainability concepts. However, P retention by pristine biochars is usually low and a modification step is always required to improve their P recovery efficiency. The pre- or post-treatment of biochars with metal salts seems to be one of the most efficient approaches. This review aims to summarize and discuss the most recent developments (from 2020- up to now) in: i) the role of the feedstock nature, the metal salt type, the pyrolysis conditions, and the experimental adsorption parameters on metallic-nanoparticles-loaded biochars properties and effectiveness in recovering P from aqueous solutions, as well as the dominant involved mechanisms, ii) the effect of the eluent solutions nature on the regeneration ability of P-loaded biochars, and iii) the practical challenges facing the upscaling of P-loaded biochars production and valorization in agriculture. This review shows that the synthesized biochars through slow pyrolysis at relatively high temperatures (up to 700–800 °C) of mixed biomasses with Ca– Mg-rich materials or impregnated biomasses with specific metals in order to from layered double hydroxides (LDHs) biochars composites exhibit interesting structural, textural and surface chemistry properties allowing high P recovery efficiency. Depending on the pyrolysis's and adsorption's experimental conditions, these modified biochars may recover P through combined mechanisms including mainly electrostatic attraction, ligand exchange, surface complexation, hydrogen bonding, and precipitation. Moreover, the P-loaded biochars can be used directly in agriculture or efficiently regenerated with alkaline solutions. Finally, this review emphasizes the challenges concerning the production and use of P-loaded biochars in a context of circular economy. They concern the optimization of P recovery process from wastewater in real-time scenarios, the reduction of energy-related biochars production costs and the intensification of communication/dissemination campaigns to all the concerned actors (i.e., farmers, consumers, stakeholders, and policymakers) on the benefits of P-loaded biochars reuse. We believe that this review is beneficial for new breakthroughs on the synthesis and green application of metallic-nanoparticles-loaded biochars.

1. Introduction

Most of phosphorus-based fertilizers used in agriculture are extracted from non-renewable phosphates rocks' natural reserves. These P-stocks are unequally distributed overall the world with more than 85% located in Morocco, the Middle East, and North African countries (Daneshgar et al., 2018). Due to the important increase in the worldwide population

* Corresponding author.
E-mail addresses: s.jelali@squ.edu.om (S. Jellali), samarhadroug@gmail.com (S. Hadroug), mwardy@squ.edu.om (M. Al-Wardy), hamed@squ.edu.om (H. Al-Nadabi), najat.nassr@rittmo.com (N. Nassr), mejdi.jeguirim@uha.fr (M. Jeguirim).

https://doi.org/10.1016/j.jenvman.2023.118307
Received 2 February 2023; Received in revised form 22 May 2023; Accepted 29 May 2023

and its food needs, it has been warned that these non-renewable P reserves would be seriously depleted by the end of the current century

precipitation, coagulation-flocculation, biological processes, membranes filtration, and adsorption (Priya et al., 2022; Witek-Krowiak

Abbreviation list/nomenclature

P	Phosphorus
WWTPs	Wastewater treatment plants (WWTPs)
USEPA	United States, Environmental Protection Agency
Mt	Million tones
Gt	Billion tones
BET	Brunauer-Emmett-Teller
pHpzc	pH of zero point charge
T	Pyrolysis temperature or adsorption experiment temperature (°C)
G	pyrolysis gradient (°C/min)
t	Residence time, or contact time (min or h)
TPV	Total pore volume (cm^3/g)
C0	Initial concentration (mg/L)
D	Biochar dose
q_{max}	Adsorption capacity
–	Not given
L	Langmuir
F	Freundlich
Ca	Calcium
Mg	Magnesium
$CaCO_3$	Calcium carbonates
$Ca(OH)_2$	Calcium hydroxide
CaO	Calcium oxide
XRD	X ray diffraction
FTIR	Fourier transform infrared
$MgCO_3$	Magnesite
$MgCl_2.6H_2O$	Magnesium chloride hexahydrate
$Mg(NO_3)_2.6H_2O$	Magnesium nitrate hexahydrate
$Mg(CH_3COO)_2{\cdot}4H_2O$	Magnesium acetate tetrahydrate
$Ca_5(PO_4)_3(OH)$	Hydroxyapatite
$CaIC_2.6H_2O$	Calcium chloride hexahydrate
$Mg_3(PO_4)_2$	Magnesium phosphates
$MgHPO_4$	Magnesium hydrogen phosphate
$Mg(H_2PO_4)_2$	Magnesium dihydrogen phosphate
$Ca_3(PO_4)_2$	Amorphous calcium phosphates
$Fe_3(PO_4)_2.8H_2O$	Vivianite
AlO(OH)	Boehmite
Al_2O_3	Aluminum oxide
H_2O_2	Hydrogen peroxide

(Cordell et al., 2009). Nowadays, crop production is essentially ensured through the use of synthetic fertilizers that are based on P, nitrogen (N) and potassium (K) (Ludemann et al., 2022). Due to their large solubility in water and low retention by agricultural soils, a relatively high proportion of the contained nutrients (i.e., P and N) may not be used by the plants and consequently reaches and pollutes the underlying groundwater and surface water bodies (Priya et al., 2022). At the same time, large quantities of P are annually being discharged in urban and industrial wastewaters since about 1 kg of P was generated per capita and by year (Witek-Krowiak et al., 2022). In the environment, P may be brought by either nonpoint sources such as water runoff and soil erosion, or point source comprising confined livestock activities and municipal or industrial wastewater treatment plants (WWTPs) (Azam et al., 2019). In WWTPs, the presence of P is mainly imputed to human excreta, industrial activities, recycling, household, and storm water with proportions of 28%, 26%, 18%, 14%, and 14%, respectively (Witek-Krowiak et al., 2022). Based on a well elaborated predictive study, van Puijenbroek et al. (2019) tried to estimate the global nutrients discharge from households to surface water bodies under different scenarios. They showed that despite nutrients removal by WWTPs will be enhanced by 10%–40% between 2010 and 2050, the P discharged amount may reach 1.6 to 2.4 million tones (Mt) by 2050. Even if typical urban treated wastewaters may contain P concentrations reaching 20 mg/L (Neal and Jarvie, 2005), it is commonly reported that dissolved P in surface waters with contents higher than 0.02 mg/L may seriously deteriorate the quality of these ecosystems (USEPA, 1995). Therefore, P discharged into urban, industrial and agricultural wastewaters, along with nitrogen compounds are considered as serious threats to water bodies since they may be responsible of the eutrophication phenomenon (L. L. Liu et al., 2021). This process may result in an important deterioration of the water bodies' physical, chemical and microbiological quality, and even mass killing of fish and other organisms due to excessive algae growth and dissolved oxygen depletion (Glibert, 2020). In the USA, the annual economic loss due to eutrophication of freshwaters was estimated to be around $2.2 billion (Dodds et al., 2009).

Numerous technologies have been developed for the removal/recovery of phosphorus from effluents. They mainly include: chemical et al., 2022). Chemical precipitation is the most applied method for P removal, where insoluble metal-phosphates precipitates are formed in presence of added metal salts such as Fe, Al, Ca, and Mg. These precipitates can be separated from the water phase by decantation or filtration but should be adequately managed later in order to avoid any negative impacts on the environment (Paul et al., 2001). Coagulation-flocculation usually uses aluminum and ferric chloride and also generates new by-products that have to be appropriately managed. Biological methods use phosphate accumulating organisms (PAO) which recovers P from wastewaters when exposed to alternate anaerobic/aerobic conditions (Daly et al., 2020). This method has several drawbacks such as high energy consumption and sensitivity to experimental conditions. Membrane filtration (i.e., reverse osmosis) is a non-selective separation process and efficiently removes P from wastewaters. However, this method is very costly due to the high energy consumption (Issaoui et al., 2022). Adsorption technology uses low cost materials and can selectively remove P from wastewater (Priya et al., 2022). It is usually recommended owing to its design simplicity, operation easiness, and effectiveness. Thus, P recovery by adsorption method and the reuse of the P-loaded material in agriculture as an eco-friendly amendment has been pointed out as a promising and attractive approach to compensate for the natural P continuous depletion (Abbas et al., 2021; Ayaz et al., 2021; Hadroug et al., 2022). Various commercial adsorbents have been used for P recovery from wastewaters such as zeolites, chitosan, and biomasses-derived materials (Italiya and Subramanian, 2022).

Huge amounts of biomasses (140 billion tones (Gt)) are annually produced in the world (Tripathi et al., 2019). Biomasses are defined as organic or non-organic solid products derived from organisms present in a given natural environment (Tursi, 2019). Depending on their sources, three types of biomasses are usually distinguished: lignocellulosic, animal, and sludge. They can be produced from agricultural, domestic, and industrial activities (Jawaid et al., 2017). If miss-managed, biomasses may represent serious threat to the human health and the environment. Until now, in the majority of developing countries, there is no clear strategy for their sustainable valorization through their reuse as organic feedstocks for energy recovery (Jellali et al., 2021b; Yilmaz and Selim,

2013), for natural polymers extraction (Zhou and Wang, 2020), as organic amendment in agriculture (Jellali et al., 2022b) and as efficient adsorbents for pollutants from aqueous and gaseous effluents (Jellali et al., 2021c). Some of these wastes have been tested as raw materials for nutrients recovery from aqueous solutions (Chakhtouna et al., 2022; Wahab et al., 2011). However, they exhibited low nutrients adsorption capacities limiting their direct possible valorization (i.e., in agriculture). In addition, the valorization of these raw materials as soil fertilizers without a pre-treatment process, to guarantee their safety, does not constitute a sustainable solution.

Biomasses can be converted into various by-products through different thermochemical methods including mainly torrefaction, gasification, hydrothermal carbonization, and slow pyrolysis (Danso-Boateng and Achaw, 2022; Jha et al., 2022). Usually, these methods permit the conversion of biomasses into three phases: bio-oil, and/or biogas, and/or a solid residue (char). The proportion of each of these phases is dependent on both feedstock properties and the used conversion technology's experimental conditions. For common thermochemical experimental conditions, the torrefaction; gasification; hydrothermal carbonization; and slow pyrolysis processes, usually favor the production of biochars; syngas; hydrochars; and bio-oil, biogas and biochars, respectively (Awasthi et al., 2023; Danso-Boateng and Achaw, 2022). The choice of using a given conversion technology is a complex process that should include simultaneously technical (feasibility and maturity of the technology), social (perception and acceptability) and economic challenges (profitability and viability) (Oladejo et al., 2019). Table 1 gives a brief definition of these thermochemical methods and their main advantages and disadvantages.

Slow pyrolysis method involves the thermal treatment of biomass in absence of oxygen. It is one of the most used thermochemical conversion methods (Garcia et al., 2022). Compared to the other thermochemical conversion technologies, pyrolysis has the main advantage of zero-wastes production since the biomass is completely transformed into fuels (bio-oil and biogas) that can be used for energetic purposes, and a carbonaceous solid residue called biochar (Buss et al., 2022; Garcia et al., 2022). The carbon in the biochar is highly recalcitrant against decomposition and its mean residence time may exceed 1000 years (Roberts et al., 2010). All dry biomasses can be pyrolyzed, such as lignocellulosic materials, animal wastes and sludge. The degree of biochars production is dependent on both the pyrolysis conditions and the nature of biomass (lignocellulosic, animal or sludge). It was reported that usually higher yields of biochar with important carbon contents, enhanced surface area and microporosity are favored for moderated pyrolysis temperatures (400–500 °C), higher heating rates (10–20 °C/min), and smaller feedstock particle size (Rangabhashiyam and Balasubramanian, 2019). Moreover, During the pyrolysis process, the inherent minerals in the feedstocks play an important role in catalyzing the biomass conversion into biochars (Giudicianni et al., 2021; Haddad et al., 2017). These same minerals existing in the produced biochars may provide the plants with the required nutrients for their growth (El-bassi et al., 2021; Haddad et al., 2021). Moreover, biochars have been identified as promising materials for carbon sequestration, greenhouse gas emissions reduction (Jellali et al., 2022b), and for the efficient removal of pollutants such as heavy metals, pesticides, pharmaceuticals, etc. From aqueous solutions (Awasthi, 2022; Jellali et al., 2021c).

Likewise, biochars were highlighted as attractive materials for sustainable agriculture, as they can be used as ecofriendly fertilizers instead of the commercial synthetic ones. When applied as amendments of agricultural soils, biochars usually increase their water retention capacity, favor the microbiological activity in the sub-soils, and improve the cultivated crops growth and yields (Allohverdi et al., 2021; Vijay et al., 2021). However, these biochars may have low mineral contents (i.e. nitrogen, phosphorus) and their enrichment with mineral nutrients is an interesting agronomic solution for improving soil fertility properties and plant growth (El-bassi et al., 2021; Haddad et al., 2021; Jellali et al., 2022b). Recent studies have clearly shown that most biochars, even when produced at high temperatures and residence times, exhibited negligible or low P adsorption capacities (Qin et al., 2023; Van Truong et al., 2023). For this reason, in order to get enhanced P recovery, pristine biochars have been modified with various techniques including the use of acidic and alkaline solutions (Luo et al., 2022). However, biochars pre- or post-modification with metal salts such as those rich in calcium, magnesium, aluminum, iron, and lanthanum have attracted huge attention owing to their excellent P adsorption capacities. Moreover, some of these metals (i.e., Fe, Ca, Mg) are essential elements for plants growth and therefore, the amendment of agricultural solid with loaded-biochars with these metals and P, may be considered as a sustainable option.

To date, 39 review papers (according to Scopus website retrieved on

Table 1
Main advantages and disadvantages of biomasses' thermochemical conversion methods (Hussin et al., 2023; Jha et al., 2022; Oladejo et al., 2019; Pathy et al., 2021; Rangabhashiyam and Balasubramanian, 2019).

Thermochemical conversion method	Definition	Advantages	Disadvantages
Torrefaction	Biomass conversion under atmospheric pressure, a temperature range of 200–300 °C, without or with limited oxygen contents	It can be regarded both as a pre-treatment and a biomass conversion technology. Low energy inputs and operational costs. Easy pelletizing of the treated biomass	Pre-drying required. By-products usually not adapted to the end-users needs. By-products not standardized to the market requirements.
Gasification	Biomass conversion under atmospheric or elevated pressures and high temperatures (650–1400 °C)	High energy efficient. Self-sustaining technology. Possibility of liquid fuel and chemical production from the generated syngas.	Not adapted for biomasses with moisture higher than 20–30%. High capital and running cost. Technology still under research and development phase. Emissions of organic and mineral pollutants. Formation of toxic pollutants.
Hydrothermal carbonization	Biomass conversion in presence of a liquid phase at temperatures of 180–250 °C and autogenic pressure (20–100 bars).	Adapted for wet biomasses. No need for a pre-drying step. Low consumed energy Improvement of the mechanical drying step. Reduction of the released organic carbon to the environment.	Slagging and fouling problems due to high ash contents. Long reaction times. Non mature technology.
Slow pyrolysis	Biomass conversion at a temperature range of 350–900 °C without or with limited oxygen contents.	Zero-waste process. Low emissions and heavy metals release. Reduction of greenhouse gas emissions.	Not adapted for wet biomasses. Technology use still in infancy stage. High capital and operational cost. Production of high carbon monoxide contents.

February 1, 2023 for review papers containing the words "biochar" AND "phosphorus" AND "adsorption" OR "recovery" in "Title, Abstract, Keywords") have been published. This number decreases to only 4 when the search was changed to "biochar" AND "phosphorus" in "Title" AND "adsorption" OR "recovery" in "Title, Abstract, Keywords". In recent years, several excellent review papers regarding P recovery from aqueous solutions by modified biochars with metal salts have been published. They give us important insights for the design of the current review paper. Yuan et al. (2020) summarized the role of the metal salt type on the enhancement of the modified biochar P adsorption capacity and the involved mechanisms. Almanassra et al. (2021) presented an interesting overview of the P adsorption isotherms, kinetic and the impact of adsorption parameters on P recovery by metal-modified biochars. B. Liu et al. (2022) reported on the nature of metal salt on P recovery and mechanisms as well as the impact of the solutions properties (i.e., pH values and presence of competing ions). Yang et al. (2023) focused on the efficiency of using La-modified biochars for P recovery from aqueous solutions. The effect of the nature of the formed La-nanoparticles on P and other oxyanions removal was assessed and the environmental application of the P-loaded La-modified biochar was reviewed. However, few articles have tried to associate the impact of the nature of the used biomass, the type of the metal salt and the pyrolysis conditions to the physico-chemical characteristics of the metallic-nanoparticles-loaded biochars and its efficiency in recovering P from aqueous solutions. Moreover, the main challenges facing the valorization of P-loaded biochars in agriculture was not appropriately discussed in these review papers. Therefore, in the current work, we reviewed the most recent studies (after 2020) related to the application of metal-modified biochars for P recovery from aqueous solutions. We tried to link the nature of the used feedstock (lignocellulosic, animal and sludge), the used metal type (Ca, Mg, Al, Fe, La, and synthesized layered double hydroxide) and the pyrolysis conditions to the properties of the modified biochars and its efficiency in recovering P. In addition, we discussed the latest developments in the valorization of these P-loaded biochars in a context of circular economy and also the main related challenges (technical, social, economic, and policy). Finally, we highlighted the limits and shortcomings of the current research as well as the future developments avenues.

2. Biochars use for phosphorus recovery from aqueous solutions

The first published study regarding the use of biochars for P recovery from aqueous solution was performed in 2011 (Chen et al., 2011). It has concerned magnetic biochars generated from the pyrolysis at different temperatures of orange peels. Since this date, various pristine and modified biochars were synthetized and used for P recovery. The used feedstocks include lignocellulosic and animal biomasses as well as sludge from WWTPs (Almanassra et al., 2021). For a smooth presentation of this section, we summarized the related scientific literature in two sub-sections: pristine and metallic-nanoparticles-loaded biochars. Moreover, the biochars performance in recovering P from aqueous solutions was interpreted through the use of the Langmuir's adsorption capacity (q_m). This parameter represents the maximum amount of P (mg) that can be retained per a unit mass of biochar (g). It is usually used as a simple and efficient parameter for the comparison of different adsorbents' performance in retaining a given pollutant (Almanassra et al., 2021; Jellali et al., 2021a, 2022a; Yang et al., 2023).

2.1. Pristine biochars

Pristine biochars usually display limited adsorption capacities of oxoanionic pollutants in general and P in particular (Wang et al., 2021; Nardis et al., 2021). At contrary, some raw biochars release P in the used adsorbate solutions (Hadroug et al., 2021; Van Truong et al., 2023). The low P recovery capacity was attributed to the presence of high amounts of negatively charged groups on their surface such as hydroxyl (–OH), and carboxylic (–COOH) (Almanassra et al., 2021). However, some biochars have exhibited non-negligible P recovery potentials under specific conditions (Antunes et al., 2022; M. Liu et al., 2022; X. Liu et al., 2022). This ability is dependent on various factors including: i) the feedstock nature and mineral composition (lignocellulosic, sludge, or rich-materials with Ca, Mg, Fe, and Al), ii) the used pyrolysis temperature, and iii) adsorption experimental conditions (Table 2). Biochars derived from Ca-rich materials generally present high P recovery efficiencies due to the P precipitation with the dissolved calcium cations from the surface of the biochars. Indeed, when pyrolyzed at relatively high temperatures, calcium carbonates ($CaCO_3$) in $CaCO_3$-rich materials is transformed into calcium hydroxide $Ca(OH)_2$ which has a higher Ca solubility. The dissolved Ca may react with P ions to form precipitates such as hydroxyapatite (J. Yang et al., 2021). In this context, relatively high P recovery efficiencies were reported for biochars generated from the pyrolysis of egg shell at 800 °C (97.0 mg g^{-1}) (J. Yang et al., 2021), of crab shells at 500 °C (164.3 mg g^{-1}) (Cao et al., 2022), and from marble waste at 800 °C (263.16 mg g^{-1}) (Deng et al., 2021). The higher P recovery efficiency observed for marble-wastes-derived biochars is imputed to its greater $Ca(OH)_2$ contents and P initial concentrations in the synthetic solutions. Moreover, owing to their richness in several metals (especially Ca, Mg, Al and Fe), some raw-sludge-derived biochars have exhibited respectable P recovery efficiencies for different types (urban or industrial) or under different pyrolysis temperatures (from 500 °C to 700 °C) (Table 2): between 23.6 and 51.8 mg g^{-1} (M. Liu et al., 2022) and from 33.2 to 56.3 mg g^{-1} (Yang et al., 2022) (Table 2).

Contrary to sludge-derived biochars, typical lignocellulosic biomasses derived biochars have usually low P recovery capacities (Almanassra et al., 2021; Van Truong et al., 2023). However, some of them such as marine algae, highly concentrated in metals, may successfully recover P from aqueous solutions (Table 2). A P adsorption capacity of 78.0 mg g^{-1} was observed for a macroalgae (*Ulva ohnoi*) from Australia. A similar behavior was mentioned for biomass residues from the Brazilian Amazon where P adsorption recovery of Palm kernel cake-, Açaí seed-, and nut-shell-derived biochars were assessed to 79.5, 92.3, and 123.5 mg $g^{-1,}$ respectively (Canteral et al., 2022). The P recovery data analysis gathered under different experimental conditions by using the principal component analysis (PCA) emphasized that this process was directly and highly associated with their mineral composition, carbon (C) contents, pH and cation exchange capacities.

For a given biomass, the pyrolysis temperature highly affects the biochars' metal composition, and textural characteristics (Li et al., 2021; Liu et al., 2022a; Zhao et al., 2022). Indeed, usually, these metal contents, surface areas, and microporosity increase with the increase of temperatures (before a possible structure collapse at around 800–900 °C)). This textural properties improvement generally results in an enhancement of P recovery performance (Li et al., 2021; Liu et al., 2022a; Zhao et al., 2022). For instance, Liu et al. (2022) showed that increasing the pyrolysis temperature of sewage sludge from 500 to 700 °C, raised the P recovery by more than 119%. Likewise, Zhao et al. (2022) reported that P recovery efficiency by biochars derived from a wetland plant "*Thalia dealbata Fraser*" was increased by more than 2.5 times when the pyrolysis temperature was increased from 300 to 700 °C. This finding is mainly induced by the biochars' physico-chemical properties enhancement. For instance, for the latter study, the Brunauer-Emmett-Teller (BET) surface area and total pore volume (TPV) was increased from 3.3 m^2 g^{-1} to 0.0036 cm^3 g^{-1} (at 300 °C) to 117.3 m^2 g^{-1}, and 0.2582 cm^3 g^{-1} (at 700 °C), respectively. However, it is clear on the basis of Fig. 1-a that there is no optimal pyrolysis temperature value for the production of biochars having high P recovery performance. This is because of the important differences in the physico-chemical properties of the feedstocks even if they belong to the same type (lignocellulosic, animal and sludge) (Fig. 1-a). Similarly, Fig. 1-b indicates that no correlation exists between the BET surface area and the P recovery capacity. For instance, for lignocellulosic biomasses, low P recovery efficiencies were observed even for high BET surface area

Table 2
Effect of the feedstock nature and pyrolysis conditions on phosphorus recovery efficiencies by pristine biochars from aqueous solutions (T = pyrolysis temperature; G = pyrolysis gradient; t = residence time; TPV: total pore volume; C0: P initial concentration; D: biochar dose; t: contact time; T: temperature; q_{max}: P-PO4 adsorption capacity; -: not given; L: Langmuir; F: Freundlich). This table does not contain data related to raw biochars with negligible P adsorption capacities.

Feedstock and provenance	Pyrolysis conditions	BET surface area (m^2g^{-1})	TPV (cm^3g^{-1})	Adsorption conditions	Isotherm	Langmuir's adsorption capacity (mg g^{-1})	Reference
Lignocellulosic-biomasses							
Wetland plant: Thalia dealbata Fraser, China	T = 300 °C; G = 8 °C/min; t = 2 h	3.3	0.0036	C0 = 5–160 mg/L; D = – g/L; pH = 7.0; t = 48 h; T = 25 °C	Langmuir	0.2	(Y. Zhao et al., 2022)
	T = 500 °C; G = 8 °C/min; t2-h	13.5	0.0078			0.4	
	T = 700 °C; G = 8 °C/min; t = 2 h	117.3	0.2582			0.5	
Wheat straw, China	T = 600 °C; G = 10 °C/min; t = 2 h	227.1	–	C0 = 1–400 mg/L; D = 7.0 g/L; pH = 6.0; t = 24 h; T = 25 °C	Langmuir	1.6	(Q. Zheng et al., 2020)
Corn straw, China	T = 400 °C; G = – °C/min; t = – h	–	–	C0 = -mg/L; D = 1 g/L; pH = –; t = – h; T = 20 °C	Langmuir	6.8	(B. Li et al., 2021)
	T = 690 °C; G = – °C/min; t = – h					7.4	
Corn straw, China	T = 600 °C; G = 4 °C/min; t = 2 h	–	–	C0 = 50–1000 mg/L; D = 2 g/L; pH = 6.0; t = 24 h; T = 25 °C	Langmuir	17.0	Ai et al. (2022)
Peanut shells, China	T = 550 °C; G = 15 °C/min; t = 2 h	153.0	0.24	C0 = 10–200 mg/L; D = 1 g/L; pH = –; t = 2 h; T = 25 °C	Langmuir	70.1	(X. Liu et al., 2022)
Macroalgae, Australia	T = 500 °C; G = 10 °C/min; t = 1 h	6.1	0.037	C0 = 300–1000 mg/L; D = 3 g/L; pH = 4.5-; t = 24 h; T = 22 °C	Langmuir	78.00	Antunes et al. (2022)
Acai seed, Brazil	T = 700 °C; G = 3.33 °C/min; t = -h	–	–	C0 = 10–300 mg/L; D = 2 g/L; pH = 8.0; t = 13 h; T = 26 °C	Langmuir	92.3	Canteral et al. (2022)
Nut shell, Brazil						123.5	
Palm kernel cake, Brazil						79.5	
Sludge							
Dewatered sludge, China	T = 700 °C; G = 2.5 °C/min; t = 0.5 h	–	–	C0 = 20–100 mg/L; D = 15 g/L; pH = 7.0; t = 24 h; T = 25 °C	Langmuir	5.5	(J. Liang et al., 2022)
Dry sludge, China	T = 500 °C; G = – °C/min; t = 1 h	13.36		C0 = 1–450 mg/L; D = 1.25 g/L; pH = 11.02; t = – h; T = 25 °C		23.6	(M. Liu et al., 2022)
	T = 700 °C; G = – °C/min; t = 1 h	20.93				51.8	
Municipal sludge, China	T = 600 °C; G = 10 °C/min; t = 2 h	–	–	C0 = 5–200 mg/L; D = 1 g/L; pH = –; t = 24 h; T = 25 °C	Langmuir	33.2	Yang et al. (2022)
Paper mill sludge, China						56.3	
Calcium-rich materials							
Egg shell, China	T = 800 °C; G = 5 °C/min; t = -h	1.60	0.016	C0 = 50–200 mg/L; D = 2 g/L; pH = –; t = 24 h; T = 25 °C	Langmuir	97.04	(J. Yang et al., 2021)
Crab shells, China	T = 500 °C; G = – °C/min; t = – h	–	–	C0 = 50–1000 mg/L; D = 1 g/L; pH = 6; t = 24 h; T = 25 °C	Langmuir	164.3	Cao et al. (2022)
				Idem, T = 30 °C		170.5	
				Idem, T = 35 °C		209.4	
Marble waste, China	T = 800 °C; G = 5 °C/min; t = 2 h	92.81	0.265	C0 = 0–300 mg/L; D = 0.3 g/L; pH = 8.0; t = 24 h; T = 25 °C	Langmuir	263.16	Deng et al. (2021)

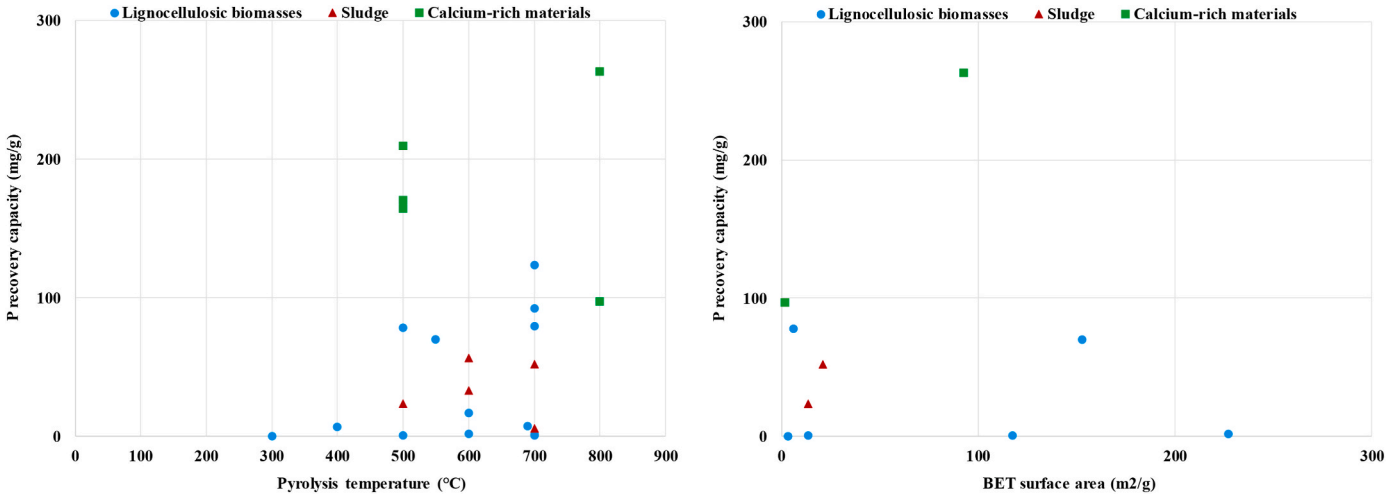

Fig. 1. Effect of the pyrolysis temperature (a) (n = 22) and surface area and (b) surface area (n = 10) on P recovery for different types of biomasses; These figures do not contain data related to materials having negligible P recovery.

(Fig. 1-b). This is also valid for calcium rich materials where the P recovery is mainly governed by precipitation rather than physical adsorption (Deng et al., 2021). The absence of correlation between the pyrolysis temperature and P recovery efficiency was also noticed in the review papers of Almanassra et al. (2021) and Jellali et al. (2022b). They imputed this behavior to the wide variation of feedstocks' intrinsic

properties.

Moreover, the used solution pH values (in comparison with the pH of zero point charge (pHzpc) of the adsorbent) as well as its temperature may have a sensitive effect on P recovery performance (Almanassra et al., 2021; Bacelo et al., 2020; Vikrant et al., 2018). For instance, Cao et al. (2022) when studying P recovery from pyrolyzed crab shells at 500 °C, showed that this efficiency increased from 164.3 mg g^{-1} at 25 °C by more than 27% at 35 °C. Similarly, the review paper of Shakoor et al. (2021) underlined four important parameters that can significantly affect biochars capacity in recovering P and ammonium: solution pH, contact time, metallic oxides contents on biochars surface, and co-occurring ions. In the current review paper, besides these parameters, the P recovery efficiency by pristine biochars appears to be mainly dependent on the feedstocks' inherent mineral contents. Materials having high Ca contents (eggshells, crab shells, marble wastes) exhibit the highest recovery capacities (Table 2). Similarly, based on an intensive review of published papers before 2021, Almanassra et al. (2021) showed that crab shells, crawfish have the best P recovery efficiencies. They also pointed out that the P precipitation with Ca cations might be the dominant involved mechanism. These biochars have, however, two main challenges: i) the high production cost since usually high temperatures (>800 °C) are needed in order to convert the Ca contained into the related feedstocks into $Ca(OH)_2$, ii) their low organic matter contents which limit their direct use for agricultural purposes. One solution could consist in the mixing of these biochars with C-rich-lignocellulosic-biomasses-derived biochars (El-bassi et al., 2021). Biochars rich in both nutrients and organic matter are necessary for the improvement of agricultural soils quality and crops growth (Z. Chen et al., 2023; Haddad et al., 2021). These economic and technical challenges will be discussed in detail in section 4.

2.2. Metallic-nanoparticles-loaded biochars

Various metal-rich products (Ca, Mg, Fe, Al, La, Ni, Zn etc.) have been used for the synthesis of metallic-nanoparticles-loaded biochars (Almanassra et al., 2021; Dai et al., 2020; Shakoor et al., 2021). Mainly, two methods were used for this operation (Fig. 2). The first one is named impregnation and consists in stirring, for a sufficient time, the feedstock (pre-modification) or the biochar (post-modification) with a solution containing the dissolved metal. The second method consists in mixing the biomass with natural or industrial materials rich in Ca, Mg, or Al. For clarity reasons, this section is divided in four separated subsections where the feedstocks were modified with different products rich with: i) Ca and/or Mg, ii) Fe and/or Al, iii) Lanthanum (La), and iv) layered double hydroxides of two different metals.

2.2.1. Modification with Ca– Mg-based products

As indicated in section 2.1, pristine biochars generated from the pyrolysis of Ca- and Mg-rich products have the highest P recovery efficiencies. This kind of feedstock are abundant in the nature, low cost and do not harm the environment (i.e. marble, eggshells, sepiolite, etc.). Two main procedures are generally used for biochars modification with Ca or Mg: (i) mixing with calcium (Ca)- magnesium (Mg)-rich products such as: $CaCO_3$ (Cao et al., 2020), $Ca(OH)_2$ (Zeng and Kan, 2022), calcium oxide (CaO) (Ai et al., 2022), eggshells (L. L. Wang et al., 2021), oyster shell (Xu et al., 2022), magnesite (Fang et al., 2022), and sepiolite (Deng et al., 2021), (ii) impregnation within Ca– Mg-aqueous solution prepared by dissolving calcium chloride (Zhuo et al., 2022), magnesium chloride (X. Liu et al., 2022), and magnesium acetate (Li et al., 2022). Biochars generated from the pyrolysis of biomasses mixed with Ca–Mg-rich materials usually exhibit high P recovery efficiency (Almanassra et al., 2021). This is mainly due to the formation of nanoparticles of CaO or $Ca(OH)_2$ and MgO or $Mg(OH)_2$. These latter nanoparticles have high pHzpc (around 12) (Tao et al., 2020) which favors the P retention through electrostatic interactions between the P anions and the positively charged biochars particles. Moreover, such modification can improve the textural properties of the generated biochars (surface area and microporosity) which may also result in P recovery enhancement through physical adsorption of P ions (Fang et al., 2022). However, P recovery by this kind of modified biochars is a complex process since different mechanisms can be involved at the same time. Therefore, in some cases, even if the textural properties are deteriorated due to a collapse of the biochars structure (for pyrolysis temperatures larger than 800 °C), higher P recovery performance may be observed (J. Yang et al., 2021). This may be due to the important contribution of the precipitation of P with Ca and Mg ions which is usually favored at high pyrolysis temperatures (Deng et al., 2021; C. Sun et al., 2022).

The P recovery efficiency seems to be dependent on various parameters including the biomass nature, the Ca– Mg-rich products type, the mass ratio between these two materials, the concentration of the modifying agents in the aqueous solutions (Ca or Mg molarity), the pyrolysis temperature as well as the adsorption conditions (i.e., solution's pH and temperature). For instance, for a constant mass ratio (biomass/eggshell) of 1:1 and pyrolysis temperature of 800 °C, P was

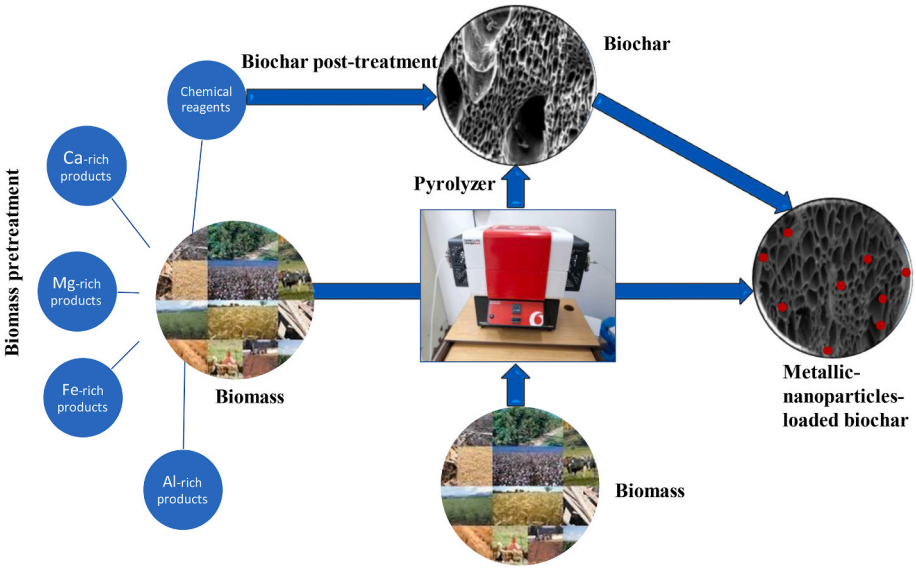

Fig. 2. Used methods for the synthesis of metallic-nanoparticles-loaded biochars.

recovered from aqueous solutions at amounts of 251.2 and only 74.9 mg g^{-1} by a lignocellulosic feedstock (sugarcane bagasse and melamine) (Liao et al., 2022), and dewatered sludge (J. Yang et al., 2021), respectively. This finding may be due to the fact that for the lignocellulosic composite biochar, the P recovery by precipitation (as hydroxyapatite: $Ca_5(OH)(PO_4)_3$) was the dominant mechanism. Furthermore, for lignocellulosic composite biochars, owing to their higher surface area and $CaO/Ca(OH)_2$ contents, better P recovery efficiencies were achieved by eggshells (Liao et al., 2022), oyster shell (Xu et al., 2022), and sepiolite (Deng et al., 2021) compared to $CaCO_3$ (Cao et al., 2020) (Table 3). Besides the higher the percentage of Ca-rich material, the higher the P recovery efficiency. For instance, Ai et al. (2022) showed that P adsorption capacities of 17, 126, 150, and 226 mg g^{-1} were measured for corn straw derived biochar post-modified with 0%, 5%, 30%, and 65% of CaO (w:w), respectively. The X ray diffraction (XRD) analyses showed that with the increase of the CaO fraction in the modified biochar, CaO and $CaCO_3$ were transformed into $Ca(OH)_2$, which contributes the most to the P recovery through precipitation (Zeng and Kan, 2022). Moreover, the XRD and FTIR analyses showed clearly that characteristics bands of $Ca(OH)_2$ have significantly vanished after P adsorption indicating their reaction with P ions and OH groups in order to form hydroxyapatite and amorphous calcium phosphate (Ai et al., 2022). Besides precipitation, which was cited as the dominant mechanism, complexation, electrostatic interaction and hydrogen bonding contribute altogether to the achievement of this relatively high adsorption capacity.

Exceptional high P recovery capacities were reported for composite biochars generated from the pyrolysis of corn stalk with eggshell at a mass ratio of 1:5 (581.0 mg g^{-1}) (C. Sun et al., 2022) and from food wastes (95% rice and 5% vegetable residues) mixed with magnesite ($MgCO_3$) at a mass ratio of 5:2 (523.9 mg g^{-1}) (Fang et al., 2022) (Table 3). This behavior was explained by the combination of several privileging factors including (Fang et al., 2022): i) the relatively low used pH (5.0) compared to the pH of zero-point charge (11.0) which favors the P anions (mainly as $H_2PO_4^-$) adsorption by the positively charged biochars particles ($\equiv MgOH^+$) through electrostatic interactions, ii) the high surface area (298.5 m^2 g^{-1}) favoring the physical adsorption of P, and iii) the high dissolution rate of Mg in the aqueous solutions contributing to the formation of Mg–P precipitate ($MgHPO_4$, $3H_2O$).

The second type of modification consisted on the use of aqueous solutions of magnesium chloride hexahydrate ($MgCl_2$,$6H_2O$) (Qingshan He et al., 2022; Lv et al., 2022; Nardis et al., 2022), magnesium acetate tetrahydrate ($Mg(CH_3COO)_2{\cdot}4H_2O$) (Li et al., 2022) and calcium chloride hexahydrate ($CalC_2$,$6H_2O$) (Feng et al., 2022; Zhuo et al., 2022). Results showed that compared to $CaCl_2$, biochars generated from modified biomasses with $MgCl_2$ solutions allow higher P recovery efficiencies (Table 3). Indeed, modified biochars with $CaCl_2$ exhibited P adsorption capacities of 24 mg g^{-1} for feedstocks of winery distillers grains and an invasive plant *Eupatorium adenophorum* residues (Feng et al., 2022), 32 mg g^{-1} for rice straw (Feng et al., 2022), and 34 mg g^{-1} for corn stover (Zhuo et al., 2022). Modified biochars with $MgCl_2$ exhibited P recovery efficiencies of 28.1 mg g^{-1} for sludge (Nardis et al., 2021), 34.5 mg g^{-1} for poultry litter (Nardis et al., 2021), 61.0 mg g^{-1} for corn straw (Zhu et al., 2020), 91.5 mg g^{-1} for peanut shells (X. Liu et al., 2022), 129.4 mg g^{-1} for *Lycium chinensis* branch filings (Li et al., 2022), 226.9 mg g^{-1} for pig manure (Nardis et al., 2022), 233.4 mg g^{-1} for *Hydrocotyle Vulgar* plant residues (Q. Liang et al., 2022), and 357.0 mg g^{-1} for bamboo pieces (Jiang et al., 2018). On the basis of Tables 3 and it can be deduced that high P recovery capacities are usually obtained for high $MgCl_2$ concentrations (>2 M). For instance, P recovery of efficiencies of 223.4 and 357.0 mg g^{-1} were obtained for $MgCl_2$ concentrations of 3 M (Jiang et al., 2018; Q. Liang et al., 2022) and 2 M (Jiang et al., 2018), respectively. This can be partially explained by the fact that this treatment favors the deposition of higher contents of Mg-based nanomaterials on the biochars surface and thus improves the biochars textural properties (surface area and microporosity). For these two modified biochars, the measured BET surface area were relatively high: 931.1 m^2 g^{-1} for the *Hydrocotyle Vulgar* plant residues (Q. Liang et al., 2022) and 377.0 m^2 g^{-1} for the for the bamboo pieces (Jiang et al., 2018), respectively. However, this trend was not reported for other studies (Nardis et al., 2021; Tran et al., 2022). For instance, Nardis et al. (2021) reported relatively low P recovery: 28.1 and 34.5 mg g^{-1} for biochars derived from sewage sludge (Nardis et al., 2021) and poultry litter (Tran et al., 2022), even if they were modified with 2.7 M and 3.3 M $MgCl_2$ solutions respectively. Simultaneously, a much higher P adsorption capacity was reported for biochars derived from peanut shell (91.5 mg g^{-1}) even if this biomass was pretreated with a lower $MgCl_2$ concentration (0.5 M) (X. Liu et al., 2022). This particular behavior may be due to the relatively high biochar's BET surface area (133.0 m^2 g^{-1}), total pore volume (0.2 cm^3/g), and richness with various functional groups, including –OH, C═C, and Mg–O, which altogether contribute to an effective P recovery from aqueous solutions. These incoherent findings prove that P process is a highly complex and may be affected at the same time by interconnected parameters including the nature and characteristics of the feedstock, the nature and concentration of the metal salt, the experimental conditions of both the pyrolysis and the adsorption experimental conditions.

It is worth mentioning that increasing the pyrolysis temperature during the synthesis of Ca– Mg-modified biochars usually enhances their P recovery capacities (Haddad et al., 2018; Jiang et al., 2018). This behavior was mainly imputed to the improvement of the biochars textural properties. Indeed, in these two studies, after the pyrolysis temperature increase, the BET surface area has increased by factors of 1.3, and more than 2, respectively. However, even if this assumption is valid for specific biomasses, there is no relationship between the pyrolysis temperature and the P recovery efficiency (n = 42) for the studied three biomasses (lignocellulosic, sludge and animal) (Fig. 3-a). Likewise, Fig. 3-b clearly shows that there was no association between the biochars' BET surface area values and their performance in recovering P from aqueous solutions (n = 33). Indeed, significant P recovery efficiency was obtained even for low BET surface area. BET surface areas values in the range of 190–280 m^2 g^{-1} were not associated with an improvement of P recovery (Fig. 3-b). However, biochars with higher BET values (between 300 and 400 m^2 g^{-1}) exhibit more important P recovery efficiencies (>344 mg g^{-1}). Another study (not presented in this figure) showed that the P recovery was evaluated to only 223 mg g^{-1} although the modified biochar has a BET surface area of more than 931 m^2 g^{-1} (Q. Liang et al., 2022).

The absence of such relationships between the P recovery efficiency and the pyrolysis temperature and/or the BET surface areas was also highlighted by (Jellali et al., 2022c) in their review paper regarding nitrates and ammonium recovery by modified biochars derived from the three common biomasses: lignocellulosic and animal biomasses and sludge. Once again, this finding may be due to the fact that, P recovery by these modified biochars is a complex process including not only physical adsorption but also precipitation (L. He et al., 2022; X. Liu et al., 2022; Tran et al., 2022; Zhuo et al., 2022). The contribution degree of each of these mechanisms varies according to the nature of the feedstock, the modification process, the pyrolysis conditions and the properties of the effluent (P. Zhang et al., 2022b). Most of the reviewed studies focused on a qualitative appreciation of these mechanisms. Further work is still needed to get a quantitative determination of the effective contribution of each one of these mechanism in the overall P recovery process. However, for various Ca– Mg-modified biochars, P recovery through precipitation has been pointed out as the dominant mechanism (Almanassra et al., 2021). The nature of the formed precipitates depends on both the properties of the biochars and the effluent. They include tri-magnesium phosphate $Mg_3(PO_4)_2$ for a Mg-post modified biochar from peanut shells (X. Liu et al., 2022), both $Mg_3(PO_4)_2$ and magnesium hydrogen phosphate ($MgHPO_4$) for a Mg-modified-corn-straw-derived biochar (Zhu et al., 2020), $MgHPO_4$

Table 3
Effect of biochars modification with calcium and magnesium rich products on phosphorus recovery efficiencies from aqueous solutions.

Feedstock and provenance	Pre-treatment conditions	Pyrolysis conditions	Post-treatment conditions	BET surface area ($m^2 g^{-1}$)	TPV ($cm^3 g^{-1}$)	Adsorption conditions	Isotherm	q_{max} (mg g^{-1})	Reference
Lignocellulosic biomasses mixing with Ca– Mg-rich materials									
Rape straw, China	Mixing with $CaCO_3$ at a mass ratio of 1:5	T = 800 °C; G = 20 °C/min; t = 1.5 h	–	32.2	0.024	C0 = 10–200 mg/L; D = 1 g/L; pH = –; t = 24 h; T = 25 °C	Langmuir	96.6	Cao et al. (2020)
Yellow pine wood, USA	Mixing with $Ca(OH)_2$ at a mass ratio of 1:1 for 24 h	T = 100 °C; G = – °C/min; t = 2 h	–	120.6	–	C0 = 100–400 mg/L; D = 1 g/L; pH = 9; t = 48 h; T = 20 °C	Langmuir	125.6	Zeng and Kan (2022)
Corn straw, China	–	T = 600 °C; G = 4 °C/min; t = 2 h	Mixing with 65% CaO solution for 3.4 h	–	–	C0 = 50–1000 mg/L; D = 2 g/L; pH = 6.0; t = 24 h; T = 25 °C	Langmuir	226.0	Ai et al. (2022)
			Mixing with 50% CaO solution for 3.4 h					329.0	
			Mixing with 30% CaO solution for 3.4 h					150.0	
			Mixing with 15% CaO solution for 3.4 h					126.0	
Corn straw, China	Mixing with eggshell at a mass ratio of 1:0.25 and 5% $CaCl_2$ solution for 18 h	T = 700 °C; G = 5 °C/min; t = 1.5 h	–	–	–	C0 = 5–125 mg/L; D = 0.3 g/L; pH = 5.3; t = 18 h; T = 25 °C	Langmuir	137.4	(L. P. Wang et al., 2021)
Corn stalk, China	Mixing with eggshell at a mass ratio of 1:5	T = 800 °C; G = – °C/min; t = 4 h	–	–	–	C0 = 0–200 mg/L; D = 0.3 g/L; pH = 6.8; t = 24 h; T = 18 °C	Langmuir	560.3	(C. Sun et al., 2022)
						Idem; T = 25 °C		581.0	
						Idem; T = 35 °C		588.6	
Sugarcane bagasse, China	Mixing with eggshell and melamine at a mass ratio of 1:1 for 1 h	T = 800 °C; G = 5 °C/min; t = 2 h	–	27.6	–	C0 = 50–100 mg/L; D = 0.02 g/L; pH = 7; t = 2 h; T = 27 °C	Langmuir	251.2	Liao et al. (2022)
Peanut shell waste, China	Mixing with oyster shell at a mass ratio of 1:1	T = 800 °C; G = – °C/min; t = 4 h	–	127.2	0.369	C0 = 0–400 mg/L; D = 0.4 g/L; pH = 6.8; t = 24 h; T = 28 °C	Langmuir	172.4	Xu et al. (2022)
Food waste, China	Mixing with $MgCO_3$ at a mass ratio of 5:2	T = 700 °C; G = 10 °C/min; t = 2 h	–	298.5	–	C0 = 50–1000 mg/L; D = 1 g/L; pH = 5.0; t = -h; T = 23 °C	Langmuir	523.9	Fang et al. (2022)
Bagasse, China	Mixing with sepiolite at a mass ratio of 1:1	T = 800 °C; G = 5 °C/min; t = 2 h	–	106.7	0.397	C0 = 0–300 mg/L; D = 0.6 g/L; pH = 8.0; t = 24 h; T = 25 °C	Langmuir	128.2	Deng et al. (2021)
Lignocellulosic biomasses impregnation with Ca– Mg-solutions									
Corn stover, China	Impregnation with 1 M $CaCl_2$ for 24 h	T = 800 °C; G = 5 °C/min; t = 1 h	–	238.30	0.133	C0 = 10–100 mg/L; D = 1 g/L; pH = 6; t = -h; T = – °C	Langmuir	33.9	Zhuo et al. (2022)
Winery distillers grains, China	–	T = 600 °C; G = 2.5 °C/min; t = – h	Impregnation with 0.1 M $CaCl_2$ solution	–	–	C0 = 20–407.16 mg/L; D = 0.5 g/L; pH = 8.0; t = 24 h; T = 15 °C	Langmuir	23.1	Feng et al. (2022)
						Idem; T = 25 °C		24.1	
						Idem; T = 35 °C		27.0	
Invasive plant: Eupatorium adenophorum, China	–	T = 600 °C; G = 2.5 °C/min; t = – h	Impregnation with 0.1 M $CaCl_2$ solution			Idem; T = 15 °C		20.5	
						Idem; T = 25 °C		24.0	
						Idem; T = 35 °C		25.7	
Rice straw, China	–	T = 300 °C; G = 2.5 °C/min; t = – h	Impregnation with 0.1 M $CaCl_2$ solution	–	–	Idem; T = 15 °C		28.0	
						Idem; T = 25 °C		31.8	
						Idem; T = 35 °C		33.0	
Corn waste, China	Impregnation with 0.02 M $MgCl_2$,$6H_2O$ for 12 h	T = 450 °C; G = 10 °C/min; t = 2 h	–	19.16	0.032	C0 = 5–1000 mg/L; D = 1 g/L; pH = –; t = 24 h; T = 25 °C	Langmuir-Freundlich	23.9	(Qingshan He et al., 2022)

(*continued on next page*)

Table 3 (*continued*)

Feedstock and provenance	Pre-treatment conditions	Pyrolysis conditions	Post-treatment conditions	BET surface area ($m^2 g^{-1}$)	TPV ($cm^3 g^{-1}$)	Adsorption conditions	Isotherm	q_{max} (mg g^{-1})	Reference
Rice husk, Vietnam	Impregnation with 3.3 M $MgCl_2$ for 2 h	T = 500 °C; G = – °C/ min; t = 1 h	–	196.04	–	C0 = 10–100 mg/L; D = 1 g/L; pH = 8; t = 2 h; T = 25 °C	Langmuir	17.1	Tran et al. (2022)
Corn cob, Vietnam				106.71				38.4	
Hass avocado, USA	–	T = 400 °C; G = –°C/ min; t = 2 h	Impregnation with 0.4 M $MgCl_2$,$6H_2O$ for 30 min	2.2	–	C0 = 5–500 mg/L; D = 3.3 g/L; pH = 6.5; t = 24 h; T = 20 °C	Langmuir	30.3	Kang et al. (2022)
			Impregnation with 0.1 M $MgCl_2$,$6H_2O$ for 30 min	1.4				39.8	
Corn straw, China	Impregnation with 0.5 M $MgCl_2$ for 4 h	T = 550 °C; G = – °C/ min; t = 0.5 h	–	273.82	0.146	C0 = 4–200 mg/L; D = 3.33 g/L; pH = 4.99; t = 24 h; T = – °C	Langmuir-Freundlich	61.0	Zhu et al. (2020)
Ground coffee waste, Korea	Impregnation with 3 M $MgCl_2$ for 18 h	T = 500 °C; G = 10 °C/ min; t = – h	–	36.4	0.11	C0 = 38–6094 mg/L; D = 2 g/L; pH = 7; t = 48 h; T = 20 °C	Langmuir	63.5	Shin et al. (2020)
spent coffee grounds, China	Impregnation in 3 M KOH solution for 4 h. Then mixing within a 0.5 $MgCl_2$ and 1 M NaOH solutions for 4 h	T = 500 °C; G = 10 °C/ min; t = 2 h	–	107.3	–	C0 = –; D = 0.5 g/L; pH = 7; t = 48 h; T = 25 °C	Langmuir-Freundlich	91.1	(D. Chen et al., 2023)
Peanut shell, China	Impregnation with 0.5 M $MgCl_2$ for 24 h	T = 550 °C; G = 15 °C/ min; t = 2 h	–	133.0	0.20	C0 = 10–200 mg/L; D = 1 g/L; pH = –; t = 24 h; T = 25 °C	Langmuir	91.5	(X. Liu et al., 2022)
Lycium chinensis branch filings, China	Impregnation with 20% $Mg(CH_3COO)_2{\cdot}4H_2O$ for overnight	T = 400 °C; G = –°C/ min; t = 2 h	–	76.59	0.08	C0 = 0.5–2000 mg/L; D = 2 g/L; pH = 7; t = 12 h; T = 23 °C	Langmuir	129.4	Li et al. (2022)
Hydrocotyle Vulgar, China	Impregnation with 3 M $MgCl_2$,$6H_2O$ for 24 h	T = 500 °C; G = 10 °C/ min; t = 2 h	–	931.1	–	C0 = -mg/L; D = 10 g/L; pH = 7; t = 24 h; T = 25 °C	Langmuir	223.4	(Q. Liang et al., 2022)
Bamboo pieces, Japan	Impregnation with 2 M $MgCl_2$ solution for 4 h	T = 400 °C; G = 10 °C/ min; t = 1 h	–	311	0.52	C0 = 19.7–498 mg/L; D = 1 g/L; pH = –; t = 90 h; T = – °C	Langmuir	344.0	Jiang et al. (2018)
		T = 500 °C; G = 10 °C/ min; t = 1 h		377	0.54			357.0	
		T = 600 °C; G = 10 °C/ min; t = 1 h		399	0.53			370.0	
Sludge mixing with Ca-rich materials									
Urban dewatered sewage sludge, China	Mixing with dolomite powder at a ratio of 1:1 for 12 h	T = 800 °C; G = 5 °C/ min; t = 2 h	–	11.31	0.03	C0 = 25–175 mg/L; D = 1.2 g/L; pH = 4.5; t = – h; T = 25 °C	Langmuir	29.2	Li et al. (2019)
Dewatered sludge, China	Mixing with limestone powder at a ratio of 1:3	T = 800 °C; G = 10 °C/ min; t = 2 h	–	–	0.106	C0 = 50–500 mg/L; D = 2 g/L; pH = 2; t = 24 h; T = 25 °C	Langmuir	231.3	Xu et al. (2022)
Activated sludge powder, China	Mixing with shell wastes at a mass ratio of 1:1 for 7 h	T = 800 °C; G = 5 °C/ min; t = 2 h	–	–	–	C0 = 50–400 mg/L; D = 0.5 g/L; pH = 7; t = 24 h; T = 25 °C	Langmuir	154.2	Li et al. (2023)
						C0 = 50.-400 mg/L; D = 0.5 g/L; pH = 7; t = 24 h; T = 35 °C		162.1	
						C0 = 50.-400 mg/L; D = 0.5 g/L; pH = 7; t = 24 h; T = 45 °C		169.6	
Dewatered sludge, China	Mixing with eggshell waste at a mass ratio of 1:2 for 0.5 h	T = 800 °C; G = – °C/ min; t = 2 h	–	44.0	0.066	C0 = 50.-200 mg/L; D = 2 g/L; pH = –; t = 24 h; T = 25 °C	Langmuir	94.9	(J. Yang et al., 2021)
	Mixing with eggshell waste at a mass ratio of 1:1 for 0.5 h			34.7	0.086			74.9	

(*continued on next page*)

Table 3 (*continued*)

Feedstock and provenance	Pre-treatment conditions	Pyrolysis conditions	Post-treatment conditions	BET surface area ($m^2 g^{-1}$)	TPV ($cm^3 g^{-1}$)	Adsorption conditions	Isotherm	q_{max} (mg g^{-1})	Reference
	Mixing with eggshell waste at a mass ratio of 2:1 for 0.5 h			34.8	0.079			106.9	
Sludge impregnation with Ca– Mg-solutions									
Sewage sludge, Brazil	Impregnation with 2.7 M $MgCl_2$ solution for 24 h	T = 500 °C; G = 10 °C/min; t = 2 h	–	–	–	C0 = 5–500 mg/L; D = 5 g/L; pH = –; t = 24 h; T = – °C	Langmuir	28.1	Nardis et al. (2021)
Activated sludge, China	Impregnation with 1.25 M $MgCl_2$,$6H_2O$ solution for 24 h	T = 600 °C; G = – °C/min; t = 2 h	–	81.17	0.272	C0 = 25–500 mg/L; D = 2 g/L; pH = 9.0; t = 24 h; T = 25 °C	Langmuir-Freundlich	142.31	(M. Zhang et al., 2021)
Sewage sludge, China	Impregnation with 0.5 M $MgCl_2$,$6H_2O$ solution for 12 h	T = 500 °C; G = 10 °C/min; t = 2 h	–	99.57	0.130	C0 = 18–360 mg/L; D = 2 g/L; pH = 3.3; t = -h; T = 25 °C	Langmuir	97.45	Jiang et al. (2022)
Animal biomasses mixing with Ca– Mg-rich materials									
Pig manure, China	Mixing with magnesium-containing desulfurization waste residue at a mass ratio of 10:3 for 8 h	T = 800 °C; G = 10 °C/min; t = – h	–	42.82	0.107	C0 = 10.-200 mg/L; D = 1 g/L; pH = 9.0; t = – h; T = – °C	Langmuir	117.78	(L. He et al., 2022)
Animal biomasses impregnation with Ca– Mg-solutions									
Poultry litter, Brazil	Impregnation with 2.7 M $MgCl_2$ solution for 24 h	T = 500 °C; G = 10 °C/min; t = 2 h	–	–	–	C0 = 5.-500 mg/L; D = 5 g/L; pH = –; t = 24 h; T = – °C	Langmuir	34.5	Nardis et al. (2021)
Pig manure, Brazil	Impregnation with 3.3 M $MgCl_2$ $6H_2O$	T = 500 °C; G = 10 °C/min; t = 2 h	–	26.9	–	C0 = 10.-10000 mg/L; D = 25 g/L; pH = –; t = 24 h; T = – °C	Langmuir	226.9	Nardis et al. (2022)

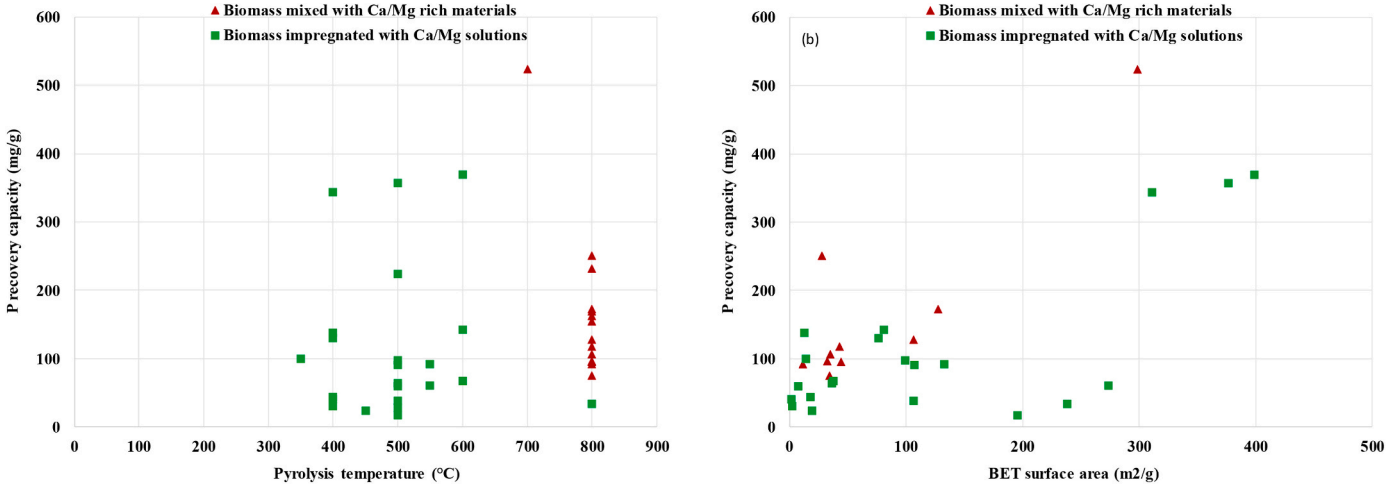

Fig. 3. Effect of the pyrolysis temperature (n = 42) (a) and surface area (n = 33) (b) on P recovery for different treatment of biomasses.

and magnesium dihydrogen phosphate ($Mg(H_2PO_4)_2$) for spent coffee grounds pretreated with potassium hydroxide (KOH), magnesium chloride ($MgCl_2$) and sodium hydroxide (NaOH); $Ca_7Mg_2P_6O_{24}$ for biochars generated from the co-pyrolysis of pig manure and magnesium-containing desulfurization waste residue (L. He et al., 2022), and $Ca_5(PO_4)_3(OH)$ and amorphous calcium phosphates ($Ca_3(PO_4)_2$) for a Ca-modified corn stover biochar (Zhuo et al., 2022). The regeneration of these P-loaded biochars and the P slowness release rate will be discussed in section 3.

The dominance of precipitation mechanism during P recovery by Ca–Mg-loaded biochars was highlighted by Yuan et al. (2020). In this review paper, the $Ca(OH)_2$ and $MgO/Mg(OH)_2$ formed after the pyrolysis at high pyrolysis temperatures are cited as the main components responsible of P recovery. For instance, for HPO_4^{2-} (at pH between 5.21 and 10.67), can be precipitated as follows (Yuan et al., 2020):

$$2SMgO\text{–}OH_2^+ + HPO_4^{2-} \leftrightarrow (SMgO)_2HPO_4 + 2H_2O \quad (1)$$

$$3HPO_4^{2-} + 5Ca^{2+} + 4OH^- \rightarrow Ca_5(PO_4)_3(OH) + 3H_2O \quad (2)$$

On the other hand, the recovery experimental conditions may play an important role in the P recovery efficiencies. Two parameters are cited as key factors for this process; aqueous pH and temperature. However, there is no specific trend of the pH effect on P recovery. Indeed, in case of the electrostatic interactions is the dominant mechanism, the lower the pH values, the higher the P adsorption performance (Shin et al., 2020; Zhuo et al., 2022). This is due to the fact that at low pH values (lower than the adsorbents' pHzpc that are generally alkaline),

the negatively charged P ions are preferentially adsorbed by the positively charged biochars particles. For example, lowering the pH from 10 to 6 has increased the P recovery efficiency by a factor of 3 for a Ca-modified corn stover biochar (Zhuo et al., 2022). However, when the precipitation mechanism is dominant compared to the electrostatic interaction, the increase of pH will, at contrary, significantly increase the P recovery efficiency (L. He et al., 2022; Kang et al., 2022; Tran et al., 2022). For instance, L. He et al. (2022) showed that the increase of pH from 5 to 10 permits the biochars generated from the co-pyrolysis of pig manure and magnesium-containing desulfurization waste residue to increase the P adsorption amount by 2.3 times. Moreover, the increase of the solution temperature is generally accompanied with significant P recovery efficiency since this reaction is generally reported to be endothermic and spontaneous (Feng et al., 2022; Tran et al., 2022). For instance, Feng et al. (2022) showed that increasing the solution's temperature from 15 to 35 °C, has increased the P adsorption by post-modified biochars with 0.1 M $CaCl_2$ from winery distillers grains, an invasive plant *Eupatorium adenophorum*, and rice straw by 17%, 25%, and 18%, respectively. A Similar trend was observed by Tran et al. (2022) for Mg-modified biochars from rice husk and corn cob. On the other hand, the presence of typical competing ions (i.e., Cl^-, SO_4^{2-} and NO_3^-) do not significantly affect P recovery by Ca-modified biochars (Ai et al., 2022; Fang et al., 2022). For instance, P recovery efficiency decreased by 2.4%, 4.9%, and 8.2% when using tap water, river water and lac water instead of distilled water, respectively (Ai et al., 2022). However, due to their high electronegativity, the presence of fluorides (F^-) could lead to a net decrease of P recovery efficiency (~29%). It is worth to mention that development of biochars through impregnation with Ca– Mg-chemical reagents is a high cost, non-eco-friendly, and complicated method. These drawbacks may seriously limit the application of this method in practice. At contrary, the synthesis of modified biochars with Ca– Mg-rich materials and its use for P recovery may be considered as an attractive and effective option. However, reducing the energetic cost of the pyrolysis process is the main challenge of this operation (see section 4). These P-loaded biochars can be used, in a context of circular economy, as slow release fertilizers for the cultivation of various plants. This aspect will be covered in section 3.

2.2.2. *Modification with Fe– Al- based products*

Iron and Aluminum nanoparticles were successfully loaded on biochars derived from lignocellulosic and animal biomasses and sludge (Almanassra et al., 2021; Shakoor et al., 2021; Yuan et al., 2020). This operation can be achieved through mixing with Fe– Al-rich-solid residues such as red mud (C. Zhang et al., 2023) or impregnation with dissolved compounds (Fe and/or Al) from industrial sludge (Van Truong et al., 2023) or water-dissolved commercial chemicals such $FeCl_3{,}6H_2O$; $Fe_2SO_4{,}7H_2O$; $AlCl_3{,}6H_2O$, $Al(NO_3)_3$, etc. (Lv et al., 2022; Phuong Tran et al., 2022; Ren et al., 2021; F. Yang et al., 2021; Q. Zheng et al., 2020) (Table 4). This modification may be done as a pretreatment step (Phuong Tran et al., 2022; Van Truong et al., 2023; Y. Zheng et al., 2020) or after the pyrolysis as a post-treatment step (Ren et al., 2021; Q. Zheng et al., 2020). These modification processes are intended to improve the properties of the biochars and consequently to enhance their capacities in recovering P from aqueous solutions. The scientific literature review points out that P recovery capacities by these Fe– Al-modified biochars depend on several parameters such as the mineral composition of the raw feedstocks, the nature of the used Fe– Al-products and the formed nanoparticles, the pyrolysis temperature, and the adsorption experimental conditions.

Depending on the modification process, different Fe-nanoparticles may be formed at the surface of the biochars. They may involve: nano-zero-valent iron (ZVI), goethite (FeOOH), hematite (Fe_2O_3), and magnetite (Fe_3O_4). The review work performed by Yuan et al. (2020) showed that the presence of these nanoparticles improves the physico-chemical properties of the related biochars and usually results in the enhancement of P recovery performance. pH was highlighted as a key parameter of P recovery. Moreover, P recovery was ensured mainly through ligand exchange between P ions and OH^-. The comparison of P recovery efficiency by these different Fe-modified-biochars as well as the role played by the inherent metals in the feedstock was not sufficiently addressed. The review of recent published papers gave interesting insights on P recovery efficiency versus the deposited Fe-nanoparticles on the synthetized biochars and the qualitative assessment of the main involved mechanisms. Indeed, the size of the formed nanoparticles on the biochars surface can have an important effect on P recovery efficiency. Generally, the smaller the nanoparticle size (i.e., ZVI), the higher the BET surface area and the lower the diffusion resistance. In this context, Qin et al. (2023) synthetized three Fe-modified biochar from lychee twig biomass. They were loaded with (ZVI), goethite, and magnetite, respectively. They showed that the ZVI-loaded biochar exhibited the highest P adsorption capacity (19.7 mg g^{-1}) due to the possible presence of P surface precipitation mechanism. The magnetite-loaded biochar has the lowest P recovery efficiency (2.9 mg g^{-1}) even if its BET surface area was relatively high (256.9 m^2 g^{-1}). Likewise, magnetite-loaded biochars were found to have the lowest P recovery capacity (9.4 mg g^{-1}) among those loaded with nanoparticles of goethite (22.1 mg g^{-1}), ferrihydrite (18.5 mg g^{-1}), and hematite (13.8 mg g^{-1}) (Zhang et al., 2020). This finding was partially explained by the fact that P adsorption by this magnetite-loaded-biochar occurs mainly through electrostatic interactions. However increasing higher magnetite nanoparticles loads on the surface of biochars (by using higher concentrations of $FeCl_3{,}6H_2O$ and $FeCl_2{,}4H_2O$) leads to more interesting P recovery capacities (Kang et al., 2022). Indeed, these authors synthetized magnetic biochars from avocado seeds with low (impregnation with 0.037 M of $FeCl_3{,}6H_2O$ and 0.05 M $FeCl_2{,}4H_2O$) and high Fe-loadings (impregnation with 4 times more concentrated. They found that the Fe-high-loaded biochar has a P adsorption capacity of 14.9 mg g^{-1}, which is 22% higher than the one of the Fe-low-loaded biochar. This behavior was imputed to: i) a significant increase of the biochars BET surface area (~3 times), and ii) the possible formation of Fe–P precipitate such as vivianite ($Fe_3(PO_4)_2{,}8H_2O$) (Y. Liu et al., 2022). Moreover, the presence of inherent mineral in feedstocks may affect the properties of the Fe-modified biochars and consequently their performance in recovering P from aqueous solutions (F. Yang et al., 2021). These authors studied P recovery from raw and $FeCl_3$-modified biochars generated from the pyrolysis of a sawdust (low mineral content: 1.4%), a sediment (high mineral content: 78.4%) and their mixture (1:1). They showed that when pre-treated with $FeCl_3$, the higher the inherent mineral content, the higher the P recovery yield. Indeed, for an initial P concentration of 40 mg/L, the pre-treated biochars derived from the sediments, the mixed biomass, and the sawdust allow P recovery yields of 100%, 73% and 61%, respectively. This finding was attributed to the fact that during the pyrolysis process, the inherent minerals could have inhibited the transformation of $FeCl_3$ into magnetite (Fe_3O_4) and promoted the generation of a crystalline structure: $Fe_4(PO_4)_3(OH)_3$.

Concerning the Al-modified biochars, it is important to mention that this pre- or post-modification process may allow the deposition of various Al-based nanomaterials (mainly as boehmite (AlO(OH)) and aluminum oxide (Al_2O_3)) and results in a significant increase of oxygen contents (Luo et al., 2022; Van Truong et al., 2023). For instance, Q. Zheng et al. (2020) post-modified a biochar derived from the pyrolysis at 600 °C of corn straw with 0.5 M solution of $AlCl_3$. The Al-modified biochars have O/C, H/C and (O + C)/N contents of 1.6, 2.0 and 1.5 times higher than the raw biochar which confirms that Al-based nanomaterials (AlOOH and Al_2O_3) were successfully deposited on the biochar surface. As for Fe, the nature of the used Al-chemicals for the modification of the biomasses may have an important effect on the formed Al-nanoparticles and consequently on P recovery efficiency from aqueous solutions (Van Truong et al., 2023). Indeed, these authors synthetized three biochars generated from the pyrolysis of pre-treated Korean pine wastes with three Al-rich solutions: i) Al concentration of 19.34 mg/L extracted from an aluminum-rich sludge (Al_2O_3 content =

Table 4
Effect of biochars modification with iron-, aluminum- and lanthanum-rich products on phosphorus recovery efficiencies from aqueous solutions.

Feedstock and provenance	Pre-treatment conditions	Pyrolysis conditions	Post-treatment conditions	BET-N_2 surface area (m^2 g^{-1})	TPV (cmg^{-1})	Adsorption conditions	Isotherm	q_{max} (mg g^{-1})	Reference
Fe–Al modified biochars									
Pinewood, USA	Impregnation with 0.55 M $FeCl_3$ solution for 2 h	T = 600 °C; G = –; t = 1 h	–	385.0		Column experiment: 1 g of biochar packed in a column (height = 5 cm; diameter = 1.6 cm). Flow rate = 1 mL/min; C0 = 1 mg/L	–	0.18	Gao and Wan (2023)
Activated sludge, China	Mixing with 110 mg Fe (II) g^{-1} of volatile solids (VS) and 88 mg of H2O2 g^{-1} of VS	T = 300 °C; G = –; t = 2 h	–	4.9	–	C0 = 23–161 mg/L; D = 15 g/L; pH = –; t = 24 h; T = –	Langmuir	2.6	Wang et al. (2020)
Avocado seeds, USA	–	T = 400 °C; G = –; t = 2 h	Impregnation in 0.148 M $FeCl_3$,$6H_2O$ and 0.2 $FeCl_2$,$4H_2O$ solution for 0.5 h and continuous adding of 0.5 M NaOH in order to keep pH > 10.	49.9		C0 = 5–500 mg/L; D = 3.3 g/L; pH = 6.5; t = 24 h; T = 20 °C	Freundlich	14.9	Kang et al. (2022)
	–		Impregnation in 0.037 M $FeCl_3$,$6H_2O$ and 0.05 $FeCl_2$,$4H_2O$ solution for 0.5 h and continuous adding of 0.5 M NaOH in order to keep pH > 10.	17.1				12.2	
Sawdust, China	Impregnation in 5 mM $FeCl_3$ for 24 h at 60 °C	T = 500 °C; G = –; t = 2 h	–	9.41	0.062	C0 = 40 mg/L; D = 2.5 g/L; pH = –; t = 8 h; T = –	–	9.8	(F. Yang et al., 2021)
Sediment, china				69.94	0.099			16.0	
Mixture sawdust and sediment at a mass ratio of 1:1, China				13.23	0.064			11.6	
lychee twig, China	–	T = 600 °C; G = 5 °C/min; t = 1 h	–	5.2	–	C0 = 5–200 mg/L; D = 5 g/L; pH = 6; t = 4 h; T = 25 °C	Freundlich Langmuir	~0	Qin et al. (2023)
	Impregnation with 1.0 mol L^{-1} $FeCl_3$ and 72% H_2SO_4 at a ratio of 1:10:5 (g:mL:mL) in an ultrasonic bath for 2 h.	T = 600 °C; G = 10 °C/min; t = 2 h	–	256.9	–			2.9	
	–	T = 600 °C; G = 5 °C/min; t = 2 h	Impregnation with 100 mL KOH (5 mol L^{-1}) and 50 mL $Fe(NO_3)_3$ (1.0 mol L^{-1}) for 1 h	6.1	–			12.3	
	Impregnation with 9 mM $FeCl_3$,$6H_2O$ solution for 24 h	T = 900 °C; G = –°C/min; t = 2 h	–	261.7	–			19.7	
hickory wood chips, USA	Impregnation with 0.1 M $FeCl_3$ solution for 1 h	T = 600 °C; G = 10 °C/min; t = 1 h	–	–	–	C0 = 15–1000 mg/L; D = 2 g/L; pH = 8.2; t = 24 h; T = –	Freundlich	11.0	(Y. Zheng et al., 2020)
	Impregnation with 0.1 M $AlCl_3$ solution for 1 h			–	–			21.7	
Bamboo wood chips, USA	Impregnation with 0.1 M $FeCl_3$ solution for 1 h			–	–		Langmuir-Freundlich	9.2	
	Impregnation with 0.1 M $AlCl_3$ solution for 1 h			–	–			15.7	
Corn straw, China	Impregnation of 2 g with a $FeCl_3$ solution (ratio Fe/biomass = 0.05) for 24 h	T = 400 °C; G = 10 °C/min; t = 1.3 h	–	–	–	C0 = 0–65 mg/L; D = 1 g/L; pH = 8.3; t = –; T = 20 °C	Langmuir	16.6	(B. Li et al., 2021)
		T = 690 °C; G = 10 °C/min; t = 1.3 h						26.1	

(*continued on next page*)

Table 4 (*continued*)

Feedstock and provenance	Pre-treatment conditions	Pyrolysis conditions	Post-treatment conditions	BET-N_2 surface area (m^2 g^{-1})	TPV (cmg^{-1})	Adsorption conditions	Isotherm	q_{max} (mg g^{-1})	Reference
Peanut shell, China	Mixing with industrial red mud at a mass ratio of 7:3	T = 900 °C; G = 10 °C/min; t = 2 h	–	110.9	0.101	C0 = 0–500 mg/L; D = 1 g/L; pH = –; t = 8 h; T = 25 °C	Langmuir	93.2	(C. Zhang et al., 2023)
Reed straw, China	–	T = 700 °C; G = 5 °C/min; t = 2 h	Impregnation in 0.1 M $Fe_2SO_4{\cdot}7H_2O$ solution for 1 h. Then adding of 1 M $NaNH_4$ solution and stirring for 30 min.	53.3		C0 = 0–250 mg/L; D = 1 g/L; pH = –; t = 24 h; T = –	Freundlich	95.2	Ren et al. (2021)
Pine residues, South Korea	Impregnation with 0.71 M recovered aluminum solution from sludge for 24 h	T = 500 °C; G = 10 °C/min; t = 0.25 h	–	208.0	–	C0 = 12.5–400 mg/L; D = 2 g/L; pH = 7; t = 48 h; T = 25 °C	Langmuir	11.9	Van Truong et al. (2023)
	Impregnation with 0.71 M of $AlCl_3$ solution for 24 h			58.3	–			1.8	
	Impregnation with 0.71 M of $Al_2(SO_4)_3$ solution for 24 h			289.3	–			14.4	
Wheat straw, China	–	T = 600 °C; G = 10 °C/min; t = 2 h	Impregnation with 0.5 M $AlCl_3$ solution for 48 h at 85 °C	169.6	–	C0 = 10–2000 mg/L; D = 7 g/L; pH = 6; t = 24 h; T = –	Langmuir	82.8	(Q. Zheng et al., 2020)
Mimosa pigra trunks, Vietnam	Impregnation with 2 M $AlCl_3$,$6H_2O$ for 6 h	T = 500 °C; G = 10 °C/min; t = 2 h	–	255.9	–	C0 = 25–200 mg/L; D = 2 g/L; pH = 4.7; t = 24 h; T = 25 °C	Freundlich	95.1	Phuong Tran et al. (2022)
Sewage sludge, China	–	T = 600 °C; G = 5 °C/min; t = 2 h	Impregnation with 0.5 M $Fe_2SO_4$3, 0.09 M NaOH, 0.02 $NaNO_3$ for 12 h at 90 °C	33.6	0.0197	C0 = 2–70 mg/L; D = 0.4 g/L; pH = –; t = 16 h; T = 25 °C	Langmuir	196.1	Lv et al. (2022)
			Impregnation with 0.5 M $Al(NO_3)_3$, 0.09 M NaOH, 0.02 $NaNO_3$ for 12 h at 90 °C	38.1	0.0186			204.1	
Perennial woody plant, China	Impregnation in 500 mL of NaCl solution (1 M) containing Fe, then Al electrodes for an applied current density of 123.91 mA cm^{-2}.	T = 600 °C; G = –; t = 1 h	–	233.3	0.13	C0 = 5–500 mg/L; D = 1 g/L; pH = 5; t = 12 h; T = 25 °C	Langmuir-Freundlich	205.7	Cui et al. (2020)
La-modified biochars									
Walnut shell, China	Impregnation with 0.5 M $LaCl_3$ for 2 h	T = 400 °C; G = – °C/min; t = 2 h	Mixing with a soil at a mass ratio of 3% (biochar:soil)	–	–	C0 = 5–150 mg/L; D = 51.5 g/L; pH = 7; t = 24 h; T = 25 °C	Langmuir	0.42	Zhao et al. (2021)
Corn cob, China	–	T = 300–400 °C; G = –; t = 1 h	Mixing with attapulgite at a mass ratio of 1:1. Then impregnation with $LaCl_3$ solution. Then pyrolysis at T = 300–500 °C, and t = 1–2 h	78.3	–	C0 = 10–1000 mg/L; D = 20 g/L; pH = –; t = 24 h; T = –	Langmuir	12.8	Yin et al. (2022)
	–		Mixing with attapulgite at a mass ratio of 1:1. Then impregnation with poly-aluminum chloride and $LaCl_3$ solution. Then pyrolysis at T = 300–500 °C, and t = 1–2 h	79.8	–			21.3	
Wetland grass: Phragmites Australis	Impregnation with 0.12 M $LaCl_3$,$7H_2O$	Hydrothermal carbonization: T = 240 °C; G = 2 °C/min; t = 10 h	–	–	–	C0 = 10–100 mg/L; D = –; pH = –; t = 12 h; T = –	Langmuir	42.2	Shang et al. (2022)
Wheat straw, China	–	T = 300 °C; G = 10 °C/min; t = 2 h	Impregnation for 24 h with 6.3 mM	–	–	C0 = 30–100 mg/L; D = 0.4 g/L;	Langmuir	71.9	Huang et al. (2022)
		T = 800 °C; G = 10 °C/min; t = 2 h	Lanthanum solution			pH = 7; t = 24 h; T = 25 °C		62.9	
Spent coffee ground,	Mixing with $NaHCO_3$ in a mass ratio of 1:1	T = 500 °C; G = – °C/min; t = 1 h	Impregnation with 5 mM of $FeCl_3.6H_2O$, 10 mM $LaCl_3.7H_2O$	0.6		C0 = 5–175 mg/L; D = 0.4 g/L; pH =	Langmuir	75.8	Akindolie and Choi (2023)

(*continued on next page*)

Table 4 (*continued*)

Feedstock and provenance	Pre-treatment conditions	Pyrolysis conditions	Post-treatment conditions	BET-N_2 surface area (m^2 g^{-1})	TPV (cmg^{-1})	Adsorption conditions	Isotherm	q_{max} (mg g^{-1})	Reference
Republic of Korea						−; t = 1 h; T = 25 °C			
Sewage sludge, China	Impregnation with La $(NO_3)_3$ for 18.5 h	T = 400 °C; G = − °C/min; t = 2 h	–	17.3	0.096	C0 = 100–500 mg/L; D = 0.1 g/L; pH = −5 t = 24 h; T = 20 °C	Langmuir	312.6	Elkhlifi et al. (2021)
						Idem. T = 25 °C		303.0	
						Idem. T = 30 °C		294.1	

65.8%), ii) from $AlCl_3$,$6H_2O$, and iii) from aluminum sulfate ($Al_2(SO_4)_3$). The BET surface areas of these three biochars were assessed to 208.0, 58.3, and 289.3 m^2 g^{-1}, respectively. This result was confirmed by the XRD analyses which showed that the modified biochar with $Al_2(SO_4)_3$ contained well-crystallized aluminum sulfate structure and boehmite. However, in case of the Al-extract and $AlCl_3$ impregnated biochar, a low degree of aluminum sulfate and gibbsite crystallinity was formed. For these reasons, the highest P recovered amount was observed for the biochar treated with $Al_2(SO_4)_3$ (14.4 mg g^{-1}) which is 21% and 700% higher than the ones observed for the biochars treated with the Al-extract from the sludge and with $AlCl_3$, respectively. Moreover, the presence of metals in the feedstocks significantly affect the functionality of the Al-modified biochars and can have positive effect on the P recovery process (Yuan et al., 2020). A similar positive effect was also observed when biochars were post-treated with Al. Indeed, compared to the pre-treatment, a post-modification enhances the homogeneous distribution of Al-nanoparticles on the biochars surface (Yuan et al., 2020). Few studies have tried to compare P recovery efficiencies of the same biomasses modified by Fe and/or Al (Lv et al., 2022; Y. Zheng et al., 2020). For instance, Y. Zheng et al. (2020) showed that Al-modified biochars exhibit higher adsorption capacities (1.7–2.0 times) than those modified with Fe (Table 4). This may be partially explained by the fact the pHzpc of Al-modified biochars (7.8–8.0) (Phuong Tran et al., 2022) is higher than the one of Fe-modified biochars (generally acidic and may be lower than 4) (Chen et al., 2022). This will favor the electrostatic interactions between the P anions and the positively charged Al-modified-biochars particles that are dominant for pH values lower than pHzpc (Jellali et al., 2022b). These same biochars when modified with Mg, exhibited much higher adsorption efficiencies than those treated with Al (4.2–7.8 times). This behavior can be attributed to the P precipitation with Mg cations dissolved from the biochars surface. A Similar trend was observed by Lv et al. (2022) who reported P recovery efficiencies of 196.1, 204.1, and 400.0 mg g^{-1} for Fe-, Al, and Mg-sewage-sludge derived biochar. It is important to mention that mixing red mud (industrial waste rich in both Fe and Al) with biomass before pyrolysis permit to achieve a relatively high P recovery efficiency (95.1 mg g^{-1}) due combined actions of the formed nanoparticles at the surface of the biochars (C. Zhang et al., 2023). XRD, XPS and FTIR analyses showed that the generated biochar contained various peaks related to Fe- and Al-based nanomaterials and the main involved mechanisms in P recovery included electrostatic interactions, complexation, ligand exchange and also precipitation as $Fe(H_2PO_4)_3$ and $Al(H_2PO_4)_3$.

It is worth mentioning that the effect of the pyrolysis temperature on P recovery efficiency by Fe-modified biochars is somehow contradictory even when using the same feedstock. For instance, B. Li et al. (2021) showed that increasing pyrolysis temperature from 400 to 690 °C of a pre-treated corn straw with $FeCl_3$,$6H_2O$, has increased the P recovery efficiency by 57.2% (Table 4). At contrary, Ren et al. (2021) when investigating P recovery by a ZVI-modified-reeds biochars at temperatures of 300, 500, 700 and 900 °C, reported that the highest recovery capacity (95.2 mg g^{-1}) was observed for the biochar produced at 700 °C even if its BET surface area (53.3 m^2 g^{-1}) was less than the half of the one measured for the biochar produced at 900 °C. This finding may be attributed to the nature and the distribution of the nano-metals formed at the surface of the biochar (i.e. ZVI, Fe_2O_3, Fe_3O_4). A similar finding was reported by Wang et al. (2020) an activated sludge derived biochar pre-treated with Fenton reagent (Fe^{2+} and hydrogen peroxide (H_2O_2)). Moreover, contradictory results were reported for the effect of aqueous pH values. Indeed, increasing the aqueous pH to values higher than the pHzpc of the modified biochars can significantly reduce the P adsorption capacities due to the inhibition of electrostatic attraction forces between P anions and biochars particles (Kang et al., 2022; F. Yang et al., 2021). An opposite effect can be observed if the recovery process is dominated by precipitation (Qin et al., 2023).

The P recovery mechanisms by Al-nanoparticles-loaded biochars was not yet fully illustrated and precisely quantified. The review works performed by Yuan et al. (2020) and by Almanassra et al. (2021) suggested that the electrostatic attraction, and the combination electrostatic attraction/precipitation are the key parameters of P recovery. However, based on specific analyzes including XRD, FTIR and XPS, recent papers show that this process may include not only electrostatic attraction, but also complexation, ion exchange and especially precipitation at high aqueous pH values (Cui et al., 2020; C. Zhang et al., 2023; Q. Zheng et al., 2020). The quantification of each of these mechanisms in the overall P recovery process as a function of the biochars properties is an interesting research topic.

2.2.3. *Modification with La-based products*

Lanthanum is a versatile element with proved applications in environment and agriculture (Cheng et al., 2021; Yang et al., 2023). It has an important affinity to various pollutants including oxyanions (Yang et al., 2023). The first study dealing with La-modified-chars use for P recovery was reported in 2014 (Dai et al., 2014). Since this date, La-modified biochars have been widely tested for P recovery and various other mineral pollutants (i.e. arsenic, fluoride, antimonite etc.) removal from aqueous solutions mainly under static conditions at laboratory scale (Yang et al., 2023). Different La-nanoparticles may be formed on the surface of biochars. They may include: $La(OH)_3$, La_2O_3, LaOCl etc. (Yang et al., 2023). The $La(OH)_3$ is the most reported La species on biochars surface (Qi He et al., 2022). Depending on the used treatment chemical reagents, La– Fe- and Mg- nanoparticles can be deposited at the same time at the surface of the biochars (Yang et al., 2023). The objective of a such treatment is to increase the P recovery efficiency through the involvement of diverse mechanisms including precipitation (Akindolie and Choi, 2023). The review of the most recent published paper on this thematic showed that the P adsorption capacity by La-modified biochars varies in a large interval (Table 4). The highest P recovery (313 mg g^{-1}) was reported by (Elkhlifi et al., 2021) for a $La(OH)_3$-doped sewage sludge derived biochar. A relatively high P adsorption capacity (75.8 mg g^{-1}) was reported by (Akindolie and Choi, 2023) for a La–Fe-modified biochar from spent ground coffee (by using

co-precipitation method). This high efficiency was observed even if this modification has decreased the surface area from 6.2 $m^2\ g^{-1}$ (raw biochar) to 0.6 $m^2\ g^{-1}$ due to the pores blocking by the formed nanomaterials. In this study, P recovery process occurred through the combination of: i) precipitation as $FeH_2P_3O_{10}$ and lanthanum pentaphosphate (LaP_5O_{14}), ii) electrostatic attraction and ligand exchange, and iii) complexation. P recovery is dependent on the feedstock nature and the used modifying agents (Table 4). For instance, adsorption capacities of around 72, 52, 13 and less than 1 mg g^{-1} were reported for a La-carbonate composite biochar of wheat straw (Huang et al., 2022), a La–Fe (hydr)oxides/montmorillonite (E. Sun et al., 2022), a La-modified-attapulgite/biochar composite (Yin et al., 2022) and a mixture of La-modified biochar of walnut shells mixed with an agricultural soil at a mass ratio of 3% (Zhao et al., 2021), respectively. La-modified biochars usually have alkaline pHzpc values which enhances P removal efficiency by electrostatic attraction (Yang et al., 2023). However, increasing the solution pH to values higher than pHzpc can significantly reduce the P recovery efficiency. For instance, rising the pH from 3 to 10 has resulted in a P adsorption decrease by a factor 7 by a Lanthanum-ammonia-modified hydrothermal biochar from a wetland grass (*Phragmites Australis*) (Shang et al., 2022). This behavior is due to the deprotonation of the biochar surface which will repulse the negatively charged P anions. A similar trend was observed by Yin et al. (2022) when investigating P recovery by solidified La- or La–Al-modified-attapulgite/biochar composite. Moreover, as for Ca-modified biochars (see section 2.2.1), he presence of SO_4^{2-}, NO_3^-, and Cl^- (at concentrations up to 500 mg/L) do not affect the P recovery by La-modified biochars (Elkhlifi et al., 2021; Shang et al., 2022; Yang et al., 2023). However, the presence of bicarbonate ion (HCO_3) could reduce the P adsorption capacity (Qu et al., 2020; Shang et al., 2022). This may be due to the possible formation of lanthanum carbonates ($La_2(CO_3)_3$) which can reduce the interactions between P and La ions. In comparison with tri-bi-valent-metal-modified biochars, the La-modified biochars seem to be less affected by the presence of HCO_3. For instance, the P recovery efficiency by an MgO-enriched-mesoporous carbons was decreased by about 45% in the presence of a 0.1 M HCO_3^- (X. X. Liu et al., 2021). Moreover, most of studies have reported that increasing the solution temperature increases the P adsorption efficiency of La-modified biochars (Qu et al., 2020; Yang et al., 2023; Y. Zhang et al., 2021). At contrary, Elkhlifi et al. (2021) showed that P adsorption capacity by a La $(OH)_3$-doped sludge derived biochar slightly decreased (~6%) when the solution temperature was increased from 20 to 30 °C. Depending on the properties of the La-modified biochars and the aqueous solutions characteristics, the P recovery may involve various mechanisms including (Yang et al., 2023): ligand exchange with La-coordinated OH^-, or CO_3^{2-}, H-bonding with functional surface groups (i.e., carboxyl), Lewis acid-based interactions, electrostatic attraction, especially at low pH values and precipitation with La^{3+} in order to form $LaPO_4$ precipitate. The formation of this precipitate is favored by its low solubility product constant (K_{sp}) value (3.7 10^{-23}) (Elkhlifi et al., 2021). The chemical equations occurring during the electrostatic attraction and precipitation are given by equations (3)–(5), respectively (Yang et al., 2023):

$$La\text{–}OH + H^+ \leftrightarrow La\text{–}OH_2^+ \quad (3)$$

$$La\text{–}\ OH_2^+ \leftrightarrow (La\text{–}\ OH_2)^+(H_2PO_4)^- \quad (4)$$

$$La^{3+} + PO_4^{3-} \rightarrow LaPO_4 \quad (5)$$

Finally, it is important to underline that La-modified biochars was successfully tested as filtering material in constructed wetlands (Shang et al., 2022). These authors showed that this material improves the P removal rate (by more than 14%), enhances the activity and growth of γ-Proteobacyeria and phosphate-accumulating organisms, and also promotes the plants photosynthesis. The valorization of P-loaded-La--modified biochars in agriculture is of a great interest in order to promote the sustainability and circular economy concepts. This topic will be developed in section 3.

2.2.4. Modified biochars with LDHs

Biochars modification by the simultaneous use of divalent (Ca^{2+}, Mg^{2+}, Ni^{2+}, Cu^{2+}, and Zn^{2+}) and trivalent metals (Al^{3+}, Cr^{3+}, and Fe^{3+}) leads to the production of functionalized biochars with layered double hydroxides (LDHs). LDHs are defined as positively charged sheets that are balanced by intercalated anions in the hydrated interlayer regions (Yuan et al., 2020). This design and composition helps the retention of oxyanions in general and P in particular through ion exchange with various anions such as NO_3^-, Cl^-, OH^- and SO_4^{2-} (P. Zhang et al., 2022b). Moreover, compared to pristine biochars, doped biochars with LDHs exhibit improved textural and surface chemistry properties (BET surface area, microporosity, pHzpc and functional groups) which resulted in efficient P recovery (Alagha et al., 2020; Q. Zheng et al., 2020). Different combinations of divalent and trivalent metals have been tested. They included: Mg/Al (Ma et al., 2022; Q. Zheng et al., 2020), Mg/Fe (Lu et al., 2022; J. Zhang et al., 2022), Ca/Fe (Missau et al., 2022), and Zn/Al (J. Zhang et al., 2022). Moreover, these LDHs may be deposited onto the biochars media before (Buates and Imai, 2020) or after the pyrolysis process (Alagha et al., 2020). Among the synthesized LDHs-modified biochars, it is often reported that Mg/Al-LDHs-modified biochars present the highest P recovery capacities (J. Zhang et al., 2022). This is due to the relatively high affinity of P towards Mg and Al and also to its more important mechanical stability (Almanassra et al., 2021; Yuan et al., 2020). In this context, relatively high P adsorption capacities were reported for Mg/Al-LDHs-modified biochars from date palm wastes fronds: 141.8 mg g^{-1} (Alagha et al., 2020), wheat straw: 153.4 mg g^{-1} (Q. Zheng et al., 2020), and rice straw: 192.0 mg g^{-1} (Buates and Imai, 2020), respectively (Table 5). This finding is attributed to the successful deposition of Mg– Al-nanoparticles on the biochars surface which contribute to the improvement of biochars' textural properties (increase of BET surface area and porosity) and surface chemistry (increase of pH of zero-point charge and functional groups richness). For instance (Q. Zheng et al., 2020), by using XRD analyses, they confirm the presence of magnesium aluminate ($MgAl_2O_4$), Mg $(OH)_2$, AlOOH and Al_2O_3 crystals on the surface of the Mg/Al-LDHs-modified biochars. Comped to the pristine biochar, the deposition of these nanoparticles has increased the BET surface area, the O/C ratio, and the pHzpc of the Mg/Al-LDHs-modified biochar by 18%, 76%, and 5.5 units, respectively. Moreover, The FTIR analyses indicated that the modified biochar contains new Mg–O and Al–O peaks which is consistent with the successful attachment of Mg- and Al-nanoparticles on the biochar surface.

The used molar ratio of bivalent/trivalent metals for the preparation of LDHs-modified biochars significantly affect their physico-chemical properties and therefore their ability in recovering P (Almanassra et al., 2021; Yuan et al., 2020). For the case of Mg/Al-LDHs-modified biochars, high P recovery rates are usually obtained for Mg/Al ratios higher than 2:1 (Almanassra et al., 2021; S. Li et al., 2021; Yuan et al., 2020). For instance (S. Li et al., 2021), investigated the use of Mg/Al-LDHs-modified biochars for Mg/Al ratios of 2:1; 3:1 and 4:1 for P recovery from aqueous solutions. They showed that the highest recovery was obtained for an Mg/Al ratio of 3:1.

On the other hand, the adsorption experimental conditions (solution's pH and temperature) can significantly influence P recovery efficiency. Indeed, higher pH values may decrease the P recovery yield due to the repulsion between the P anions and the negatively charged LDHs-modified biochars. For instance, Missau et al. (2022), reported a P decrease by 47% when the pH solution was increased from 2 to 10. Moreover, the increase of the solution temperature usually results in higher P recovery efficiency (Alagha et al., 2020; Missau et al., 2022). For instance, increasing the solution temperature from 25 to 45 °C has resulted in P increase of 17% and 26% for functionalized biochars with Ca/Fe-LDHs, and Mg/Al-LDHs, respectively (Alagha et al., 2020; Missau et al., 2022). It is worth mentioning that as for Ca– Mg- and La-modified

Table 5
Use of layered double hydroxide-biochar composites for phosphorus recovery efficiencies from aqueous solutions.

Feedstock and provenance	Pre-treatment conditions	Pyrolysis conditions	Post-treatment conditions	BET-N_2 surface area (m^2 g^{-1})	TPV (cm^3/g)	Adsorption conditions	Isotherm	q_{max} (mg g^{-1})	Reference
Almond shell China	–	T = –°C; G = – °C/min; t = – h	Impregnation with 0.3 M $MgCl_2$ and 0.1 M $AlCl_3$	4.5	0.023	C0 = 0–200 mg/L; D = 15 g/L; pH = 6.5; t = – h; T = 30 °C	Langmuir	6.1	(S. Li et al., 2021)
Cattail biomass powder, China	–	T = 500 °C; G = – °C/min; t = 2 h	Impregnation with 0.4 M $MgCl_2$ and 0.2 M $AlCl_3$	47.3	–	C0 = 5–80 mg/L; D = 0.5 g/L; pH = 7.2; t = 24 h; T = 25 °C	Langmuir	35.2	(J. Zhang et al., 2022)
			Impregnation with 0.4 M $ZnCl_2$ and 0.2 M $AlCl_3$	18.6	–			55.8	
			Impregnation with 0.4 M $MgCl_2$ and 0.2 M $FeCl_3$	77.3	–			50.6	
Apple wood, Iran	–	T = 600 °C; G = – °C/min; t = 1 h	Impregnation with 0.03 M $MgCl_2$,$6H_2O$ and 0.01 M $AlCl_3$,$6H_2O$	40.9	0.167	C0 = 25–200 mg/L; D = 2 g/L; pH = –; t = 2 h; T = 22 °C	Langmuir	55.6	Azimzadeh et al. (2021)
Eucalyptus saligna sawdust, Brazil	–	T = 500 °C; G = 15 °C/min; t = 2 h. Then activation with CO2 at 900 °C	Impregnation with 1.5 M CaCl2 and 0.75 M FeCl3	156.3	–	C0 = 25–50 mg/L; D = 1 g/L; pH = 2.15; t = 4 h; T = 25 °C	Freundlich	98.2	Missau et al. (2022)
Date palm waste fronds, Saudi Arabia	–	T = 700 °C; G = 3 °C/min; t = 4 h	Impregnation with 4.0 M H12MgN2O12 and 4.9 M Al(NO3) 3·9H2O	441.1	0.299	C0 = 10–50 mg/L; D = 0.125 g/L; pH = 6.0; t = 24 h; T = 25 °C	Langmuir	141.8	Alagha et al. (2020)
						Idem; T = 35 °C		177.9	
						Idem; T = 45 °C		180.5	
Wheat straw, China	–	T = 600 °C; G = 10 °C/min; t = 2 h	Impregnation with 0.5 M MgCl2 and 0.5 M AlCl3	268.5	–	C0 = 1–400 mg/L; D = 7.0 g/L; pH = 6.0; t = 24 h; T = 25 °C	Langmuir	153.40	(Q. Zheng et al., 2020)
Rice straw, Japan	Impregnation with 0.03 M MgCl2 and 0.01 M AlCl3	T = 475 °C; G = – °C/min; t = 2 h	–	–	–	C0 = 25–500 mg/L; D = 2 g/L; pH = 3.0; t = 24 h; T = –°C	Langmuir	192.0	Buates and Imai (2020)

biochars, the presence of classical ions such as Cl^-, NO_3^-, and HCO_3^- at typical concentrations did not significantly affect the P adsorption by LDHs-modified biochars (Alagha et al., 2020; Buates and Imai, 2020). This is an important asset in case of application of such materials for nutrients recovery from real wastewaters.

The P recovery by LDHs-modified biochars occurs through combined mechanisms (Fig. 4). They mainly include (Q. Zheng et al., 2020): i) exchange of ligands or anions such as OH^-, Cl^-, NO_3^-, etc; ii) electrostatic interactions (protonated and positive if the pH is lower than pHpzc and negative otherwise); iii) complexation with functional groups of the biochar, and iv) precipitation with cations such as Al^{3+}, Fe^{3+}, Zn^{2+}, Ca^{2+} and Mg^{2+}. Precipitation seems to be responsible of the highest P recovered fraction especially for alkaline media (Yuan et al., 2020). Various formed precipitates were reported on the basis of XRD and XPS analyses. They include struvite ($MgNH_4PO$,$6H_2O$) and Mg $(H_2PO_4)_2$ for an Mg/Fe modified NaY zeolite (Lu et al., 2022), Mg $(H_2PO_4)_2$ for a Mg/Al rice straw modified biochar (Buates and Imai, 2020), and Mg/Al date palm waste derived biochar (Alagha et al., 2020), and $AlPO_4$ and $Mg_3(PO_4)_2$ for Mg/Al wheat straw modified biochars (Q. Zheng et al., 2020). It is important to mention that the calcined LDHs have a structure memory effect and can undergo a reconstruction of hydrotalcite structure in aqueous media. During this operation, P may be adsorbed in the interlayers (Yuan et al., 2020; Q. Zheng et al., 2020).

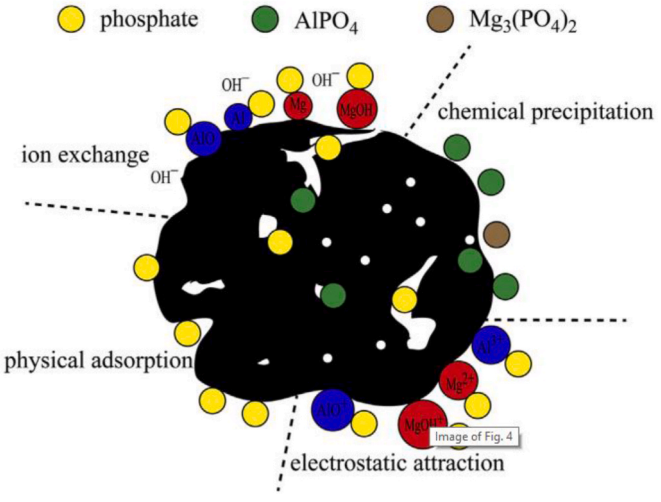

Fig. 4. Main involved mechanisms during P recovery by Mg/Al-LDHs-loaded biochars (Q. Zheng et al., 2020).

Finally, LDHs-modified biochars usually have higher P recovery efficiency than their bulk counterparts (P. Zhang et al., 2022b; Q. Zheng et al., 2020). This is because of the more microporous structure of the LDHs-modified biochars which ensures a larger contact surface between P and the sorption active sites and a reduction of the diffusion pathway before P retention. Moreover, macropores usually act as bulk buffering reservoirs for the solution to shorten the diffusion distances to the pores interfaces. However, the mesopores and micropores allow large surface areas for P transfer and retention by the active sites (P. Zhang et al., 2022b). As an example, Q. Zheng et al. (2020) showed that Mg/Al-LDHs-modified biochar has a P adsorption capacity of 153.4 mg g-1 which is 1.9 and 15.9 times higher than Al- and Mg-modified biochars, respectively.

The P recovery from all the cited above metallic-nanoparticles-

loaded biochars is a complex process that depends on several parameters regarding mainly the biochars characteristics and the adsorption experimental conditions. To promote the sustainability and circular economy concepts, these P-loaded biochars should be reused in agriculture. Therefore, it is important to find suitable solutions permitting an effective and slow release of P from these P-loaded biochars. More details about the valorization of P-loaded biochars are given in the following section 3.

3. P-loaded biochars regeneration and application

Two options have been explored at lab scale for the management of P-loaded biochars (Fig. 5). The first one consists on their regeneration by using specific eluent solutions and their subsequent reuse for other adsorption/desorption cycles. The second option consists on their direct application as slow release fertilizer for the growth of plants.

3.1. Regeneration

P desorption from the P-loaded-metal-modified biochars has been studied in batch mode using various regeneration solutions including distilled water, acidic, alkaline and salty solutions. The desorption efficiency is dependent on: i) the nature of this desorbing solution (type and concentration), ii) the properties of the modified biochar, and iii) the involved reactions during P adsorption. The use of distilled water for the regeneration of P-loaded biochars has usually led to low P desorption efficiencies (lower than 10%) (Feng et al., 2022; Nardis et al., 2021, 2022; Van Truong et al., 2023). For this reason, several studies have tested chemical solutions such as acidic, alkaline, and salty solutions. Highly acidic and alkaline solutions were generally preferred since for low pH values (<2), phosphorus exists as H_3PO_4 (uncharged) which will hinder the impact of electrostatic interactions with the negatively charged P ions. Likewise, for pH values higher than 12 (>pHzpc of the modified biochars), the P ions exist as PO_4^{3-} and consequently is repelled by the negatively charged biochars surface. Besides, there will be an important competition between the OH^- and the PO_4^{3-} on the limited number of adsorption sites.

Different acidic solutions were used such as citric acid ($C_6H_8O_7$) (Nardis et al., 2021; Shin et al., 2020; Van Truong et al., 2023), hydrochloric acid (HCl) (An et al., 2022), and a mixture of sulfuric acid (H_2SO_4) and HCl (Nardis et al., 2021, 2022). The corresponding desorption yields (at the first cycle) depend on the type of the biochar: For a 2% citric acid solution, they were assessed to be 90%, and only 26–27% for Mg-modified poultry litter and pig-manure derived biochars, respectively (Shin et al., 2020). A desorption percentage of 60% was reported when using the same eluent for an Al-modified-Korean-pine-residue-derived biochar (Van Truong et al., 2023). Alkaline solutions (especially sodium hydroxide (NaOH)) have been intensively used for the regeneration P-loaded biochars (Alagha et al., 2020; D. Chen et al., 2023; Cui et al., 2020; Fang et al., 2022; Fu et al., 2022; X. Liu et al., 2022; Missau et al., 2022; C. Sun et al., 2022; Wang et al., 2020; Y. Zhang et al., 2022). These solutions are highly efficient compared to the other acidic solutions, reaching more than 98% for a desorbing solution of NaOH (1 M) and a magnesium-doped spent coffee derived biochar (D. Chen et al., 2023). Relatively high percentages (>90%) were also reported by Wang et al. (2020); Cui et al. (2020); X. Liu et al. (2022); X. Liu et al. (2022) when exploring the P desorption from a sludge derived biochar with 0.25 M NaOH solution, from a γ-Al_2O_3/Fe_3O_4-modified-woody-plant derived biochar with 0.01 M NaOH solution, and from a Mg-modified-peanut-shell biochar and 3 M NaOH, respectively. Metal salts (i.e., (potassium chloride (KCl), sodium chloride (NaCl)) have been also used for from the regeneration of P-loaded-modified biochars (Qin et al., 2023; Zhao et al., 2021). The reported P desorption efficiencies were relatively low compared to the use of acidic or alkaline solutions. Indeed, the corresponding P desorption efficiencies were evaluated to be: only 2% (Zhao et al., 2021) for 0.01 M KCl and La-modified biochar; between 3% and 17% for 0.1 M NaCl and three Fe-modified biochars (Qin et al., 2023).

During this regeneration process, P desorption efficiency observed at the first adsorption/desorption cycle may significantly decrease with the increase of the number of regeneration cycles (Fang et al., 2022; Qin et al., 2023; Y. Zhang et al., 2022). For instance, the P desorption from a P-loaded-amino-hybrid-biopolymer-decorated magnetic biochar composites derived from green tea wastes by 0.1 M NaOH, decreased from 99.5% (first cycle) to 88.4% in the fifth cycle (P. Zhang et al., 2022b). Moreover, Fang et al. (2022) showed that the P desorption efficiency with 5 M NaOH solution from Mg-modified-food-wastes derived biochar decreased from 99.9% in the first cycle to 51.2% during the second cycle and only 42.6% after 5 cycles. Contrarily, other studies have proven that no significant decrease was observed even after 5 adsorption/desorption cycles (Cui et al., 2020; Fu et al., 2022; X. Liu et al., 2022; Wang et al., 2020). This behavior may be attributed to the fact that the adsorption occurred mainly through physical mechanisms making their adsorption and desorption relatively easier. Moreover, the desorption efficiency is dependent on the concentration of the regeneration solution. For instance, Chen et al. (2023) when studying the P desorption from a magnesium-doped spent coffee derived biochar, showed that P efficiencies of 98%, 88%, and 79%, were obtained for NaOH concentrations of 1 M, 0.5 M, and 0.2 M, respectively.

On the other hand, P desorption efficiency is dependent on the mechanisms involved during the adsorption process. Indeed, these efficiencies are very high (>99%) when the P was mainly adsorbed by

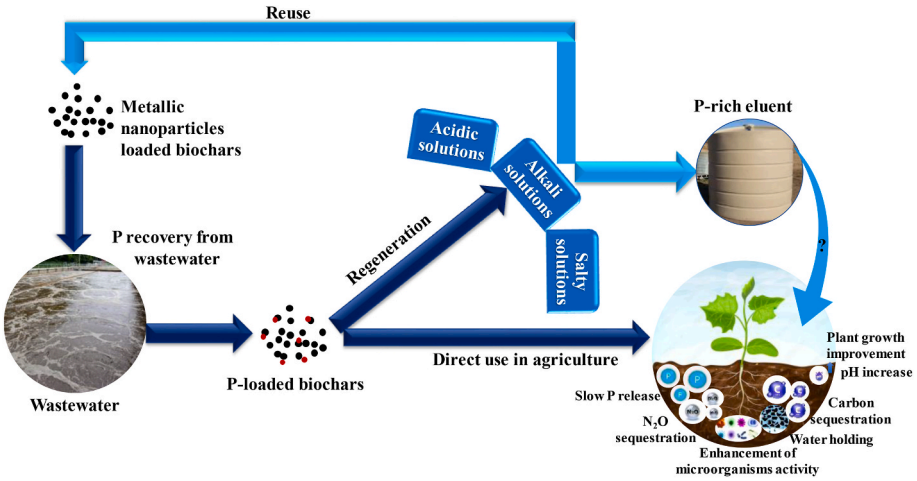

Fig. 5. Management options of P-loaded biochars.

physical processes (Y. Zhang et al., 2022), and only 2–3% when, at contrary, when P was essentially retained by chemical reactions (Qin et al., 2023; Zhao et al., 2021). Moreover, the type of the biochar should be also taken into consideration. Indeed, even for the same desorbing solution (NaCl) and the same concentration (0.1 M), the observed P desorption efficiency during the first desorption cycle was evaluated to be 17%, 11%, and 3% for lychee twig derived biochars that are modified with three different iron materials: magnetite, goethite, and zero-valent iron, respectively (Qin et al., 2023). Furthermore, Nardis et al. (2022) showed that the P desorption efficiency by an acetic acid solution increased from 20% for a Al-modified-pig-manure-derived biochar to 100% when the same biochar was pre-treated with Mg. This finding was imputed to the lower binding energy of P–Mg. Similar trend was observed for raw- MgO- and α-Fe_2O_3/MgO- modified-rice-straw biochars where P desorption efficiencies by 0.1 M HCl solution were assessed to be 92%, 83% and 80%, respectively (An et al., 2022).

It can be concluded that alkaline solutions (especially NaOH) have the highest regeneration capabilities of P-loaded biochars. However, the choice the alkaline eluent type and its concentration should take into account not only the desorption efficiency but also its economic cost and environmental impact. Further research works are needed in order to provide a cost benefit analysis of the suggested solution as well as to ensure an eco-friendly management of the P-rich eluent solutions (i.e., reuse in agriculture after specific treatment) (Fig. 5). Moreover, up to now, only few studies have tried to investigate the adsorption/desorption of P from P-loaded-metal-modified biochars under dynamic conditions (i.e., columns or reactors) (D. Chen et al., 2023; Gao and Wan, 2023; J. Zhang et al., 2022). Appreciation of P dynamic behavior is essential for an optimized upscaling of the found results at laboratory scale.

3.2. Direct application

The direct application of P-loaded biochars instead of synthetic fertilizers can improve the overall fertilization operation efficiency. Indeed, the richness of these biochars in carbons and nutrients can significantly enhance the agricultural soils' physico-chemical and microbiological properties (Z. Chen et al., 2023). These benefits contribute to the implementation of sustainable and eco-friendly agriculture. P-loaded valorization for plants growth was mainly carried out under controlled laboratory-scale conditions. Most of these assays reported that the P-loaded biochars addition has generally positive effects on seeds germination as well as plants growth (Fang et al., 2022; Gao and Wan, 2023; Nardis et al., 2021; Qin et al., 2022; Wang et al., 2020; Xu et al., 2022; J. Zhang et al., 2022; M. Zhang et al., 2023; Z. Zhao et al., 2022). For instance, the controlled bioassay showed that the seed germination rate of *Chenopodium quinoa* has increased from 80.0% (control group) to 96.7% in the presence of P-loaded Ca/Fe-rich biochar (Zhang et al., 2023b). Moreover, the average shoot length of these seedlings in presence of biochar was more than 57% longer than the one of the blank assay. A Similar trend was observed for P-loaded of: iron granular pinewood derived biochar (Gao and Wan, 2023), iron-rich sludge derived biochar (Wang et al., 2020), and ball-milled distillers grains derived biochar (Z. Zhao et al., 2022). In pot mode, Nardis et al. (2021) showed that, compared to a synthetic fertilizer (triple superphosphate: TSP), Mg-modified biochars derived from poultry litter, pig manure and sewage sludge has significantly promoted maize growth and the accumulation of P in this plant. A comparable finding was reported for the growth of corn in an agricultural soil amended with Ca-rich biochar derived from dewatered municipal sludge (Qin et al., 2022) and Chinese cabbage planted in a local soil amended with P-loaded biochars derived from the co-pyrolysis of food wastes and magnesite (Fang et al., 2022). This improvement is attributed to the well-developed structural and textural properties of the P-loaded biochars allowing them to act as slow release fertilizer and to alleviate land quality degradation. Their use as amendment in agricultural soils have various proven benefits such as improvement of the soils' water holding capacity, organic and mineral matter contents, and microbial activity (Z. Chen et al., 2023; Jellali et al., 2022b; Wang et al., 2022). Elkhlifi et al. (2021) showed that the application of P-loaded-La-modified-sludge biochars improved both soil-phosphate retention and ryegrass growth. Besides the fact that the P leaching risks in alkaline soils led to reduce its retention and availability to plants, it depends on various soil factors, including soil pH, Fe/Al oxides, clay minerals, cation exchange capacity and organic matter. It was showed in this study that the P-loaded biochar could be used as a potential substitute for synthetic fertilizers as the treatment positively affected the characteristics of the post-harvest alkaline soil, such as pH, electrical conductivity, cation exchange capacity, soil organic matter, and phosphate contents (Elkhlifi et al., 2021).

It is important to underline that despite the positive results regarding the use of P-loaded biochars use as slow release fertilizers, the relationship between the system components soil-water-plant is still not adequately assessed. Further work is needed in order to address the knowledge gaps related to the environmental impacts and safety issues related to the consumption of the amended plants' fruits. Other social, economic and policy challenges have to be seriously addressed too.

4. Challenges of P recovery by metallic-nanoparticles-loaded biochars and use

P recovery from aqueous solutions by metallic-nanoparticles-loaded biochars and reuse in agriculture can be considered as an eco-friendly approach that may contribute in resolving the energy-water-food nexus challenges. However, the appropriation and widespread application of a such approach is facing technical, social, economic and policy challenges (Fig. 6).

4.1. Technical challenges

The quality of the biochars depends on various parameters including the feedstock nature, the pyrolysis conditions and the used metal salts. Mixing lignocellulosic biomass with Ca- or Mg-rich-mineral materials and their pyrolysis at relatively high temperatures (>800–900 °C) allows interesting P recovery capacities. However, at this temperature range, a large fraction of the nutrients initially contained in the organic feedstock can be lost through evaporation. To avoid this effect, the lignocellulosic biomass can be mixed with previously calcined Ca- or Mg-rich-mineral materials and then pyrolyzed at lower temperatures (~500 °C). Moreover, the pyrolysis temperature should be carefully chosen in order to avoid any negative effects on the environment (Xiang

Fig. 6. Challenges facing P recovery by metallic-nanoparticles loaded biochars and use.

et al., 2021). Indeed, biochars produced at temperatures lower than 400 °C may contain high amounts of polycyclic aromatic hydrocarbons and those synthesized at high temperatures have high ash and low nutrients contents (Pathy et al., 2021). At contrary, biochars produced at temperatures of about 500 °C usually have ordered aromatic carbon structure and can significantly immobilize toxic elements (i.e., heavy metals). Another important technical challenge consists in the effective separation of the P-loaded biochars from the aqueous solutions for any further planned use. This separation step is a hard task for most of pristine and modified biochars. Two solutions may be applied/optimized in order to overcome this difficulty: i) biochars magnetization through treatment with Iron compounds, and ii) biochars granulation into homogenous pellets by mechanical compaction with or without a binder. Moreover, a particular attention should be paid to the metals leaching from the P-loaded-metallic-nanoparticles biochars during their direct valorization in agriculture as slow release fertilizers (Murtaza et al., 2023). Indeed, some toxic metals (i.e., Al) may be released from these biochars and contribute to the pollution of the water-soil-plant system.

On the other hand, as developed in the above sections, nutrients recovery from synthetic solutions by some metallic-nanoparticles-loaded biochars may be efficient at laboratory scale. This efficiency can significantly drop when using real wastewater and/or large dynamic pilots (columns or continuous stirring tank reactors) (Jellali et al., 2016). Therefore, the optimization and application of this dynamic P recovery process from wastewater in a real-time scenario (i.e., small villages or agro-food industries) is highly recommended. This process may also be applied at very local scale (decentralized systems) for nutrients (P and nitrogen) recovery from urine (households, educational institutions, hotels, business hubs, etc.). In that case, the most technological challenge is to separate, gather and store urine since the majority of these entities have mixed systems of grey and black water (Pathy et al., 2021). Moreover, in the developing countries, the wastewater infrastructure is very poor and not maintained, and huge efforts are needed to upgrade this sanitization system.

4.2. Social perception challenges

Few studies have focused on farmers' acceptability of producing and using biochars as amendment in agriculture (Fytili and Zabaniotou, 2018; Latawiec et al., 2017; Niemmanee et al., 2019). These studies showed that most of farmers have positive attitude towards biochars use as amendments. However, more tailored dissemination and communications tools are needed to improve their knowledge and awareness about biochars production systems as well as their environmental and economic benefits. For instance, a survey (258 households) carried out in the Amphawa district (Thailand) showed that about 77% of the farmers lack: i) knowledge about biochars manufacturing methods, and ii) awareness of agronomic benefits. More than 94% of the farmers judged insufficient the publicized media about biochars valorization in agriculture. Similar trends were observed in Africa (Rogers et al., 2022) and in Europe too (Latawiec et al., 2017).

It is worth mentioning that to ensure a long term social acceptability of P-loaded biochars production and use, citizen in general and consumers of agricultural products derived from the use of biochars as amendment, should be systemically targeted in such communication and dissemination campaigns. These events should emphasize on (Pathy et al., 2021): i) P natural reserves non-renewability, worldwide distribution and especially its current high depletion, ii) P-loaded biochars fertilization potential and its importance in the promotion of environmental sustainability and circular economy concepts, and iii) quality and safeness of the agricultural products derived from amended soils with these biochars. A specific attention should be paid to the latter aspect in order to overcome some consumers perception that such agricultural products usually carry toxic elements (Rogers et al., 2022).

4.3. Economic challenges

Phosphorus recovery from wastewaters by biochars in general and metallic-nanoparticles-loaded biochars, in particular is still an emerging research field. Economic studies are needed to support the implementation of related industrial pilots. It is noteworthy to mention that biochar market has significantly increased during the last decade. In 2021, the annual produced biochars amounts in China, Europe, USA, and Australia are evaluated to be more than 300,000; 50,000; 20,000; and 5000 tones, respectively (Garcia et al., 2022). To sustain this market growth in the future, huge efforts are needed for the reduction of biochars production cost. Indeed, this cost varies in a large interval ($0.7/kg to $17.8/kg) and depends on several factors including feedstock nature, pyrolysis temperature and the used materials/chemical for the modification process (P. Zhang et al., 2022a). However, it is usually assumed that for pyrolysis temperatures between 400 and 700 °C, this cost was in the range of $0.7/kg to $1.0/kg for sewage sludge and $1.0/kg to $1.3/kg for lignocellulosic biomass (P. Zhang et al., 2022a). A relatively low cost ($0.2/kg) was reported for a Ca-laden biochar generated from the slow pyrolysis of peanut shell and eggshells (Liu and Lv, 2023). A further reduction of biochar production cost is expected to ensure an important worldwide growth of the market and its related industries' competitiveness. This may include two options: i) reduction of the energy consumption during the pyrolysis process through the recycling of the produced bio-oil and biogas for heating the pyrolyzer, and ii) the use of natural and wasted mineral-rich materials instead of chemical reagents for the modification of the raw biomasses.

It is important to underline that until now there is no standardized economic assessment of the economic profitability of biochars production and use (Campion et al., 2023). Economic benefits assessment should include besides the reduction of expenses related to commercial fertilizers use, indirect gains such as wastewater quality improvement, water resources preservation against pollution, greenhouse gas emissions reduction (from agricultural soils and from synthetic fertilizers production plants), carbon sequestration, water capacity retention and organic matter contents increase, and heavy metals and organic pollutants immobilization in soils (Campion et al., 2023).

Finally, the commercialization of the nutrients-loaded-biochars might be challenging. To find a solution for such challenge, the social stigma of this product (derived from solid wastes and wastewater) should be resolved and the current pristine biochar popularity should be consolidated.

4.4. Policy challenges

The international biochar initiative (IBI) (IBI, 2015) and recently the European biochar certificate (EBC) (EBC, 2022) have suggested quality standards related to the properties of the feedstocks, the pyrolysis process conditions, and the biochar characteristics. For instance, for the biochar quality, the EBC targeted several physico-chemical parameters including the organic carbon content (C_{org}), the molar ratios H/C_{org} and O/C_{org}, and nutrients, heavy metals, polychlorobiphenyls and polychlorinated dibenzo-p-dioxins and furans contents etc. However, until now, biochars are not in the centre of national policymakers' attention in most the countries (Pourhashem et al., 2019). This is mainly due to the non-monetization of the ecosystem services provided by biochars (i.e., water and air quality improvement, greenhouse gas emission reduction, etc.) and a lack of communication and coordination between scientists and local stakeholders and policymakers.

To overcome the biochars' policy challenges, governments, national dedicated institutions and local stakeholders need to be aware of the threats of excessive depletion of the non-renewable P resources and the opportunities of using nutrients-loaded biochars in agriculture in the energy-water-food nexus (Pathy et al., 2021). They should be motivated and have the willingness to support an ordered transition from the use of the commercial non-renewable fertilizers to green and eco-friendly

biofertilizers generated from renewable nutrients sources (i.e., biochars). As a consequence, they will support the different stages included in the production and application of P-loaded biochars in agriculture as slow release fertilizers. This support may include: i) the implementation of specific regulations regarding the production and use of biochars in agriculture and/or ii) offering incentives to companies producing biochars as well supporting farmers (Pourhashem et al., 2019).

The coordination between all the concerned national actors should be ensured and regularly monitored. This is justified by the fact that the proposed strategy includes several different actions such as: biomass collection, preparation and modification, biomass pyrolysis, biochars use for nutrients recovery from wastewaters, and nutrients-loaded biochars application in agricultural field. This overall strategy would be compromised if any of these steps is not correctly performed.

5. Conclusions and future perspectives

In this review, most recent studies (after 2020) on P recovery by pristine and metallic-nanoparticles-loaded biochars were summarized and discussed. The effect of the feedstock inherent metal content, the nature of the impregnating metal (Ca, Mg, Fe, Al, La and LDHs), the pyrolysis conditions (temperature), and the used adsorption experimental parameters (pH, temperature, presence of competing anions) was reviewed. The regeneration and the valorization of the P-loaded biochars in agriculture were also considered. Finally, the challenges of this kind of biochar synthesis and application in a context of circular economy was discussed.

The P recovery efficiency by pristine biochars is mainly dependent on its inherent mineral contents. Materials having high contents of Ca (eggshells, crab shells, marble wastes) and Mg (sepiolite, magnesite) performed the highest recovery capacities. However, these materials should be mixed with organic-matter-rich-products if they will be valorized later in agriculture in order to compensate their organic matter poorness. Regarding metallic-nanoparticles-loaded biochars, different metal-based products were used. They include mainly Ca-, Mg-, Fe-, Al-, La- based products and mixture of them. It should be mentioned that it is challenging to make a comparison of P recovery efficiency between these different metallic-nanoparticles-loaded biochars due to the various used feedstocks and wide different range of experimental pyrolysis and adsorption conditions. However, it is clear that biochars generated from organic biomasses mixed with Ca– Mg-rich products (i.e. eggshells, sepiolite) are found to have the best P recovery capacities (higher than 500 mg g^{-1}). LDHs-modified biochars derived from the pre- or post-treatment of biomasses/biochars with metals mixture exhibited also relatively high P adsorption capacities owing to their developed structure and texture. Recovery performances of about 200 mg g^{-1} were achieved for Mg/Al solutions with concentrations ratios of more than 2:1. However, most of the LDHs-decorated biochars are synthesized by using expensive chemical reagents which hinders the real application of such materials. For biochars loaded with Fe-, Al- and La-nanoparticles, their P recovery efficiency is usually lower compared to LDHs-modified biochars and are confronted to the same real upscaling problematic (use of chemical reagents). Therefore, for practical reasons, it is recommended to synthesize metallic-nanoparticles-loaded biochars by mixing biochars from abundant biomasses (i.e., agricultural wastes) that are produced at low temperatures (~500 °C) with previously calcined Ca- or Mg- wastes. Such mixed product will be rich in $Ca(OH)_2$ and $Mg(OH)_2$, that are essential for a good P recovery, and also in organic matter. The reuse of these P-loaded biochars in agriculture as eco-friendly and slow release fertilizer will promote sustainability and circular economy concepts.

Besides the metallic-nanoparticles-loaded biochars physico-chemical properties, the P recovery efficiency is sensitive to the used adsorption experimental conditions, especially the pH, the temperature and the presence of competing anions. An increase in pH solution can induce a significant enhancement of P recovery if precipitation is the main involved mechanism. However, if the recovery process involves mainly physical adsorption (i.e. electrostatic attraction and ligand exchange), the P recovery could be seriously reduced due to the electrostatic repulsion between the P anions and the negatively charged biochars particles. Moreover, the P recovery efficiency is generally described as endothermic, spontaneous and feasible process. The presence of classic anions (nitrates, chlorides, sulfates) seems to not significantly compete with the P anions. However, a specific attention should be paid for effluents rich in carbonates and fluorides that can significantly reduce P recovery performance. The P recovery process includes various mechanisms such as electrostatic attraction (for aqueous pH values lower than pHzpc), ligand and ion exchange, hydrogen bonding, complexation and precipitation. The contribution of each of these mechanisms in the overall adsorption process is not yet precisely elucidated and further work is needed by feedstock and by impregnation agent types.

Regarding P-loaded biochars regeneration, it was well established that NaOH alkaline solution exhibited the highest efficiency compared to acidic and salty solutions. However, the sustainable management of these alkaline solutions rich in P is not yet resolved and more research works are required to manage their safe reuse in agriculture. The direct application of P-loaded biochars as slow release fertilizer in agriculture have proved that they can significantly improve the physical, chemical and biological properties of the amended soils and also plants growth and yields. However, real application of these biochars is still subjected to various challenges that can be related to: i) technical feasibility that is mainly linked to the biochar quality and its effective separation from wastewater after P adsorption; ii) economic viability associated to the relatively high production cost and commercialization of the P-loaded biochars, iii) social perception and acceptability due to lack of knowledge and awareness about biochars production systems, benefits and sanitary risks, and iv) policy constraints linked to both non-monetization of the ecosystem services provided by biochars and a lack of communication and coordination between the concerned actors (scientists, stakeholders and policymakers).

In addition, the environmental sustainability is key factor when considering the use of metallic-nanoparticles-loaded biochars for P recovery from wastewaters. Firstly, the biomass feedstock as well as the pyrolysis temperature should be carefully selected in order to avoid the production of biochars with high contents of heavy metals, polycyclic aromatic hydrocarbons, dioxins, and environmentally persistent free radicals. Secondly, the modified biochars should be selective P-adsorbents with minimal impacts on wastewaters quality (i.e., pH, electrical conductivity, hardness, etc.). Moreover, the P desorption from the Ca- or Mg–P formed precipitates can be a difficult process under natural conditions (i.e., irrigation water) due to the fact that P is buried inside the structure of this precipitate. Even if the use of alkaline solutions for P desorption was shown to be effective and permits the reuse of the adsorbent for another adsorption/desorption cycle, this approach is not recommended due to the absence of proven eco-friendly management of this desorbing solution. Finally, when valorized in agriculture, a particular attention should be given to the possible toxicity of P-loaded biochars to the soils' living organisms and cultivated plants. In this context, the biochar dose should be meticulously chosen in order to avoid significant release of toxic metals (i.e., Al) and a high increase of the soils' pHs values.

Despite that an intensive work has been already carried out regarding the synthesis and reuse of metallic-nanoparticles loaded biochars, researchers have to address the following gaps.

- Optimization of biochars synthesis process. This step should be multi-objectives including both P recovery efficiency and overall cost production. The experimental parameters to be optimized may include the: i) inherent mineral content of the feedstock, ii) the mass ratio of feedstock: Ca/Mg rich-product or the metal solution concentration, and the iii) pyrolysis temperature;

- Comparison of P recovery efficiency by biochars derived from the pyrolysis under the same conditions of a given local feedstock but treated with different metal salts;
- Evaluation of the effect biochars modification with several metal salts on P recovery performance;
- Application of the optimized metal-loaded biochars under closer conditions to real cases. In this context, the use of real effluents as well as dynamic flow conditions (continuous stirring reactors and columns) instead batch assays with synthetic solutions, is highly recommended.
- Efficient separation of the P-loaded biochars from wastewater. The test of magnetic biochars is a priority;
- Detailed assessment of the percentage contribution of each of the involved mechanisms in the overall P recovery process;
- Precise determination of P slowness release from the P-loaded-biochars mixed with agricultural soils in dynamic mode. During these long-term assays, it would be of great interest to find out links between the plant growth and the sub-soil microbiological activity;
- Quantification of metals (i.e., Al) and other components release and their effects on the system soil-water-plant;
- Test of using magnetic biochars for P recovery and also organic pollutants (i.e., pesticides, pharmaceuticals) oxidation;
- Continue working on the best ways to resolve the economic, social and policy challenges facing the widespread of biochars production and use for nutrients recovery from wastewater and reuse in agriculture.

Funding

This work was supported by Sultan Qaboos University (TRC project: RC/RG-DVC/CESR/21/01), CERTE, Tunisia, Rittmo- Agro-environnement, and Materials Science Institute, France (national projects).

Credit author statement

All authors contributed to the study conception and design. Material preparation, data collection and analysis were performed by Jellali, Hadroug and Jeguirim. The first draft of the manuscript was written by Jellali, Hadroug, Nassr and Jeguirim. All authors read and approved the final manuscript.

Ethics approval

Not applicable.

Declaration of competing interest

The authors declare that they have no known competing financial interests or personal relationships that could have appeared to influence the work reported in this paper.

Data availability

Data will be made available on request.

Acknowledgments

Authors would like to thank Sultan Qaboos University, Oman; Water Research and Technologies Centre, Tunisia; Rittmo- Agro-environnement, France, and Materials Science Institute, France for contributing to the funding of this work.

References

Abbas, F., Hammad, H.M., Anwar, F., Farooque, A.A., Jawad, R., 2021. Transforming a valuable bioresource to biochar , its environmental importance , and potential applications in boosting circular bioeconomy while promoting sustainable agriculture. Sustain. Times 13, 2599. https://doi.org/10.3390/su13052599.

Ai, D., Ma, H., Meng, Y., Wei, T., Wang, B., 2022. Phosphorus recovery and reuse in water bodies with simple ball-milled Ca-loaded biochar. Sci. Total Environ. 860, 160502 https://doi.org/10.1016/j.scitotenv.2022.160502.

Akindolie, M.S., Choi, H.J., 2023. Fe12Lao19 fabricated biochar for removal of phosphorus in water and exploration of its adsorption mechanism. J. Environ. Manag. 329, 117053 https://doi.org/10.1016/j.jenvman.2022.117053.

Alagha, O., Manzar, M.S., Zubair, M., Anil, I., Mu'azu, N.D., Qureshi, A., 2020. Comparative adsorptive removal of phosphate and nitrate from wastewater using biochar-MgAl LDH nanocomposites: coexisting anions effect and mechanistic studies. Nanomaterials 10, 336. https://doi.org/10.3390/nano10020336.

Allohverdi, T., Mohanty, A.K., Roy, P., Misra, M., 2021. A review on current status of biochar uses in agriculture. Molecules 26, 5584. https://doi.org/10.3390/molecules26185584.

Almanassra, I.W., Mckay, G., Kochkodan, V., Ali Atieh, M., Al-Ansari, T., 2021. A state of the art review on phosphate removal from water by biochars. Chem. Eng. J. 409, 128211 https://doi.org/10.1016/j.cej.2020.128211.

An, X., Chen, Y., Ao, M., Jin, Y., Zhan, L., Yu, B., Wu, Z., Jiang, P., 2022. Sequential photocatalytic degradation of organophosphorus pesticides and recovery of orthophosphate by biochar/α-Fe2O3/MgO composite: a new enhanced strategy for reducing the impacts of organophosphorus from wastewater. Chem. Eng. J. 435, 135087 https://doi.org/10.1016/j.cej.2022.135087.

Antunes, E., Vuppaladadiyam, A.K., Kumar, R., Vuppaladadiyam, V.S.S., Sarmah, A., Anwarul Islam, M., Dada, T., 2022. A circular economy approach for phosphorus removal using algae biochar. Clean. Circ. Bioeconomy 1, 100005. https://doi.org/10.1016/j.clcb.2022.100005.

Awasthi, M.K., 2022. Engineered biochar: a multifunctional material for energy and environment. Environ. Pollut. 298, 118831 https://doi.org/10.1016/j.envpol.2022.118831.

Awasthi, M.K., Sar, T., Gowd, S.C., Rajendran, K., Kumar, V., Sarsaiya, S., Li, Y., Sindhu, R., Binod, P., Zhang, Z., Pandey, A., Taherzadeh, M.J., 2023. A comprehensive review on thermochemical, and biochemical conversion methods of lignocellulosic biomass into valuable end product. Fuel 342, 127790. https://doi.org/10.1016/j.fuel.2023.127790.

Ayaz, M., Feizienė, D., Tilvikienė, V., Akhtar, K., Stulpinaitė, U., Iqbal, R., 2021. Biochar role in the sustainability of agriculture and environment. Sustain. Times 13, 1–22. https://doi.org/10.3390/su13031330.

Azam, H.M., Alam, S.T., Hasan, M., Yameogo, D.D.S., Kannan, A.D., Rahman, A., Kwon, M.J., 2019. Phosphorous in the environment: characteristics with distribution and effects, removal mechanisms, treatment technologies, and factors affecting recovery as minerals in natural and engineered systems. Environ. Sci. Pollut. Res. 26, 20183–20207. https://doi.org/10.1007/s11356-019-04732-y.

Azimzadeh, Y., Najafi, N., Reyhanitabar, A., Oustan, S., Khataee, A.R., 2021. Modeling of phosphate removal by Mg-Al layered double hydroxide functionalized biochar and hydrochar from aqueous solutions. Iran. J. Chem. Chem. Eng. 40, 565–579. https://doi.org/10.30492/ijcce.2020.38042.

Bacelo, H., Pintor, A.M.A., Santos, S.C.R., Boaventura, R.A.R., Botelho, C.M.S., 2020. Performance and prospects of different adsorbents for phosphorus uptake and recovery from water. Chem. Eng. J. 381, 122566 https://doi.org/10.1016/j.cej.2019.122566.

Buates, J., Imai, T., 2020. Biochar functionalization with layered double hydroxides composites: preparation, characterization, and application for effective phosphate removal. J. Water Process Eng. 37, 101508 https://doi.org/10.1016/j.jwpe.2020.101508.

Buss, W., Wurzer, C., Manning, D.A.C., Rohling, E.J., Borevitz, J., Mašek, O., 2022. Mineral-enriched biochar delivers enhanced nutrient recovery and carbon dioxide removal. Commun. Earth Environ. 3, 1–11. https://doi.org/10.1038/s43247-022-00394-w.

Campion, L., Bekchanova, M., Malina, R., Kuppens, T., 2023. The costs and benefits of biochar production and use: a systematic review. J. Clean. Prod. 137138 https://doi.org/10.1016/j.jclepro.2023.137138.

Canteral, K.F.F., Dias, Y.N., Fernandes, A.R., 2022. Biochars from agro-industrial residues of the Amazon: an ecological alternative to enhance the use of phosphorus in agriculture. Clean Technol. Environ. Policy. https://doi.org/10.1007/s10098-022-02427-6.

Cao, H., Wu, X., Syed-Hassan, S.S.A., Zhang, S., Mood, S.H., Milan, Y.J., Garcia-Perez, M., 2020. Characteristics and mechanisms of phosphorous adsorption by rape straw-derived biochar functionalized with calcium from eggshell. Bioresour. Technol. 318, 124063 https://doi.org/10.1016/j.biortech.2020.124063.

Cao, L., Ouyang, Z., Chen, T., Huang, H., Zhang, M., Tai, Z., Long, K., Sun, C., Wang, B., 2022. Phosphate removal from aqueous solution using calcium-rich biochar prepared by the pyrolysis of crab shells. Environ. Sci. Pollut. Res. 29, 89570–89584. https://doi.org/10.1007/s11356-022-21628-6.

Chakhtouna, H., Benzeid, H., Zari, N., Qaiss, A. el kacem, Bouhfid, R., 2022. Recent advances in eco-friendly composites derived from lignocellulosic biomass for wastewater treatment. Biomass Convers. Biorefinery. https://doi.org/10.1007/s13399-022-03159-9.

Chen, B., Chen, Z., Lv, S., 2011. A novel magnetic biochar efficiently sorbs organic pollutants and phosphate. Bioresour. Technol. 102, 716–723. https://doi.org/10.1016/j.biortech.2010.08.067.

Chen, D., Yin, Y., Xu, Y., Liu, C., 2023. Adsorptive recycle of phosphate by MgO-biochar from wastewater : adsorbent fabrication , adsorption site energy analysis and long-term column experiments. J. Water Process Eng. 51, 103445 https://doi.org/10.1016/j.jwpe.2022.103445.

Chen, Y., Hassan, M., Nuruzzaman, M., Zhang, H., Naidu, R., Liu, Y., Wang, L., 2022. Iron-modified biochar derived from sugarcane bagasse for adequate removal of aqueous imidacloprid: sorption mechanism study. Environ. Sci. Pollut. Res. 30, 4754–4768. https://doi.org/10.1007/s11356-022-22357-6.

Chen, Z., Liu, T., Dong, J.F., Chen, G., Li, Z., Zhou, J.L., Chen, Z., 2023. Sustainable application for agriculture using biochar-based slow-release fertilizers: a review. ACS Sustain. Chem. Eng. 11, 1–12. https://doi.org/10.1021/acssuschemeng.2c05691.

Cheng, M., Wang, L., Zhou, Q., Chao, D., Nagawa, S., He, D., Zhang, J., Li, H., Tan, L., Gu, Z., Huang, X., Yang, Z., 2021. Lanthanum(III) triggers AtrbohD- and jasmonic acid-dependent systemic endocytosis in plants. Nat. Commun. 12, 1–12. https://doi.org/10.1038/s41467-021-24379-z.

Cordell, D., Drangert, J.O., White, S., 2009. The story of phosphorus: global food security and food for thought. Global Environ. Change 19, 292–305. https://doi.org/10.1016/j.gloenvcha.2008.10.009.

Cui, Q., Xu, J., Wang, W., Tan, L., Cui, Y., Wang, T., Li, G., She, D., Zheng, J., 2020. Phosphorus recovery by core-shell γ-Al2O3/Fe3O4 biochar composite from aqueous phosphate solutions. Sci. Total Environ. 729, 138892 https://doi.org/10.1016/j.scitotenv.2020.138892.

Dai, L., Wu, B., Tan, F., He, M., Wang, W., Qin, H., Tang, X., Zhu, Q., Pan, K., Hu, Q., 2014. Engineered hydrochar composites for phosphorus removal/recovery: lanthanum doped hydrochar prepared by hydrothermal carbonization of lanthanum pretreated rice straw. Bioresour. Technol. 161, 327–332. https://doi.org/10.1016/j.biortech.2014.03.086.

Dai, Y., Wang, W., Lu, L., Yan, L., Yu, D., 2020. Utilization of biochar for the removal of nitrogen and phosphorus. J. Clean. Prod. 257 https://doi.org/10.1016/j.jclepro.2020.120573.

Daly, I., Jellali, S., Mehri, I., Reis, M.A.M., Freitas, E.B., Oehmen, A., Chatti, A., 2020. Phosphorus and ammonium removal characteristics from aqueous solutions by a newly isolated plant growth-promoting bacterium. Environ. Technol. 41 https://doi.org/10.1080/09593330.2019.1575917.

Daneshgar, S., Callegari, A., Capodaglio, A.G., Vaccari, D., 2018. The potential phosphorus crisis: resource conservation and possible escape technologies: a review. Resources 7, 37. https://doi.org/10.3390/resources7020037.

Danso-Boateng, E., Achaw, O.W., 2022. Bioenergy and Biofuel Production from Biomass Using Thermochemical Conversions Technologies—A Review. AIMS Energy. https://doi.org/10.3934/energy.2022030.

Deng, W., Zhang, D., Zheng, X., Ye, X., Niu, X., Lin, Z., Fu, M., Zhou, S., 2021. Adsorption recovery of phosphate from waste streams by Ca/Mg-biochar synthesis from marble waste, calcium-rich sepiolite and bagasse. J. Clean. Prod. 288, 125638 https://doi.org/10.1016/j.jclepro.2020.125638.

Dodds, W.K., Bouska, W.W., Eitzmann, J.L., Pilger, T.J., Pitts, L., Riley, A.J., Schloesser, J.T., Thornbrugh, D.J., Pitts, K.L., 2009. Policy analysis policy analysis eutrophication of U . S . Freshwaters : damages. Environ. Sci. Technol. 43, 12–19. https://doi.org/10.1021/es801217q.

EBC, 2022. Eurpean Biochar Certificate- Guidelines for a Sustainable Production of Biochar. 'Carbon Standards International (CSI), Frick, Switzerland. from. http://european-biochar.org. (Accessed 8 December 2022).

El-bassi, L., Amine, A., Jellali, S., Akrout, H., Marks, E.A.N., Matei, C., Jeguirim, M., 2021. Application of olive mill waste-based biochars in agriculture : impact on soil properties , enzymatic activities and tomato growth. Sci. Total Environ. 755, 142531 https://doi.org/10.1016/j.scitotenv.2020.142531.

Elkhlifi, Z., Kamran, M., Maqbool, A., El-Naggar, A., Ifthikar, J., Parveen, A., Bashir, S., Rizwan, M., Mustafa, A., Irshad, S., Ali, S., Chen, Z., 2021. Phosphate-lanthanum coated sewage sludge biochar improved the soil properties and growth of ryegrass in an alkaline soil. Ecotoxicol. Environ. Saf. 216, 112173 https://doi.org/10.1016/j.ecoenv.2021.112173.

Fang, Y., Ali, A., Gao, Y., Zhao, P., Li, R., Li, X., Liu, J., Luo, Y., Peng, Y., Wang, H., Liu, H., Zhang, Z., Pan, J., 2022. Preparation and characterization of MgO hybrid biochar and its mechanism for high efficient recovery of phosphorus from aqueous media. Biochar 4, 40. https://doi.org/10.1007/s42773-022-00171-0.

Feng, Q., Chen, M., Wu, P., Zhang, X., Wang, S., Yu, Z., Wang, B., 2022. Simultaneous reclaiming phosphate and ammonium from aqueous solutions by calcium alginate-biochar composite: sorption performance and governing mechanisms. Chem. Eng. J. 429, 132166 https://doi.org/10.1016/j.cej.2021.132166.

Fu, X., Wang, P., Wu, J., Zheng, P., Wang, T., Li, X., Ren, M., 2022. Hydrocotyle vulgaris derived novel biochar beads for phosphorus removal: static and dynamic adsorption assessment. J. Environ. Chem. Eng. 10, 108177 https://doi.org/10.1016/j.jece.2022.108177.

Fytili, D., Zabaniotou, A., 2018. Circular economy synergistic opportunities of decentralized thermochemical systems for bioenergy and biochar production fueled with agro-industrial wastes with environmental sustainability and social acceptance: a review. Curr. Sustain. Energy Reports 5, 150–155. https://doi.org/10.1007/s40518-018-0109-5.

Gao, A.L., Wan, Y., 2023. Iron modified biochar enables recovery and recycling of phosphorus from wastewater through column filters and flow reactors. Chemosphere 313, 137434. https://doi.org/10.1016/j.chemosphere.2022.137434.

Garcia, B., Alves, O., Rijo, B., Lourinho, G., Nobre, C., 2022. Biochar: production, applications, and market prospects in Portugal. Environments 9, 1–21. https://doi.org/10.3390/environments9080095.

Giudicianni, P., Gargiulo, V., Grottola, C.M., Alfè, M., Ferreiro, A.I., Mendes, M.A.A., Fagnano, M., Ragucci, R., 2021. Inherent metal elements in biomass pyrolysis: a review. Energy Fuel. 35, 5407–5478. https://doi.org/10.1021/acs.energyfuels.0c04046.

Glibert, P.M., 2020. Harmful algae at the complex nexus of eutrophication and climate change. Harmful Algae 91, 101583. https://doi.org/10.1016/j.hal.2019.03.001.

Haddad, K., Jeguirim, M., Jellali, S., Guizani, C., Delmotte, L., Bennici, S., Limousy, L., 2017. Combined NMR structural characterization and thermogravimetric analyses for the assessment of the AAEM effect during lignocellulosic biomass pyrolysis. Energy 134. https://doi.org/10.1016/j.energy.2017.06.022.

Haddad, K., Jeguirim, M., Jellali, S., Thevenin, N., Ruidavets, L., Limousy, L., 2021. Biochar production from Cypress sawdust and olive mill wastewater: agronomic approach. Sci. Total Environ. 752, 141713 https://doi.org/10.1016/j.scitotenv.2020.141713.

Haddad, K., Jellali, S., Jeguirim, M., Ben Hassen Trabelsi, A., Limousy, L., 2018. Investigations on phosphorus recovery from aqueous solutions by biochars derived from magnesium-pretreated cypress sawdust. J. Environ. Manag. 216, 305–314. https://doi.org/10.1016/j.jenvman.2017.06.020.

Hadroug, S., Jellali, S., Amine, A., Marzena, A., Helmi, K., James, H., 2022. Valorization of salt post - modified poultry manure biochars for phosphorus recovery from aqueous solutions : investigations on adsorption properties and involved mechanism. Biomass Convers. Biorefinery 4333–4348. https://doi.org/10.1007/s13399-021-02099-0.

Hadroug, S., Jellali, S., Jeguirim, M., Kwapinska, M., Hamdi, H., Leahy, J.J., Kwapinski, W., 2021. Static and dynamic investigations on leaching/retention of nutrients from raw poultry manure biochars and amended agricultural soil. Sustain. Times 13, 1–26. https://doi.org/10.3390/su13031212.

He, L., Wang, D., Wu, Z., Li, S., Lv, Y., 2022a. Journal of Water Process Engineering Co-pyrolysis of pig manure and magnesium-containing waste residue and phosphorus recovery for planting feed corn. J. Water Process Eng. 49, 103146 https://doi.org/10.1016/j.jwpe.2022.103146.

He, Qingshan, Li, X., Ren, Y., 2022b. Analysis of the simultaneous adsorption mechanism of ammonium and phosphate on magnesium-modified biochar and the slow release effect of fertiliser. Biochar 4, 1–16. https://doi.org/10.1007/s42773-022-00150-5.

He, Qi, Zhao, H., Teng, Z., Wang, Y., Li, M., Hoffmann, M.R., 2022c. Phosphate removal and recovery by lanthanum-based adsorbents: a review for current advances. Chemosphere 303, 134987. https://doi.org/10.1016/j.chemosphere.2022.134987.

Huang, Y., He, Y., Zhang, H., Wang, H., Li, W., Li, Y., Xu, J., Wang, B., Hu, G., 2022. Selective adsorption behavior and mechanism of phosphate in water by different lanthanum modified biochar. J. Environ. Chem. Eng. 10, 107476 https://doi.org/10.1016/j.jece.2022.107476.

Hussin, F., Nadira, N., Khalil, M., Kheireddine, M., 2023. Environmental life cycle assessment of biomass conversion using hydrothermal technology : a review. Fuel Process. Technol. 246, 107747 https://doi.org/10.1016/j.fuproc.2023.107747.

IBI, 2015. Standardized product definition and product testing guidelines for biochar that is used in soil V2.1. Int. Biochar Initiat 1–48.

Issaoui, M., Jellali, S., Zorpas, A.A., Dutournie, P., 2022. Membrane technology for sustainable water resources management: challenges and future projections. Sustain. Chem. Pharm. 25, 100590 https://doi.org/10.1016/j.scp.2021.100590.

Italiya, G., Subramanian, S., 2022. Role of emerging chitosan and zeolite-modified adsorbents in the removal of nitrate and phosphate from an aqueous medium: a comprehensive perspective. Water Sci. Technol. 86, 2658–2684. https://doi.org/10.2166/wst.2022.366.

Jawaid, Mohammad, Paridah, M.T., Saba, Naheed, 2017. Introduction to biomass and its composites. In: Jawaid, M., Md Tahir, P., Saba, N. (Eds.), Composites Science and Engineering, Lignocellulosic Fibre and Biomass-Based Composite Materials. Woodhead publisshing, pp. 1–11. https://doi.org/10.1016/B978-0-08-100959-8.00001-9.

Jellali, S., Azzaz, A.A., Al-Harrasi, M., Charabi, Y., Al-Sabahi, J.N., Al-Raeesi, A., Usman, M., Al Nasiri, N., Al-Abri, M., Jeguirim, M., 2022a. Conversion of industrial sludge into activated biochar for effective cationic dye removal: characterization and adsorption properties assessment. Water (Switzerland) 14, 2206. https://doi.org/10.3390/w14142206.

Jellali, S., Azzaz, A.A., Jeguirim, M., Hamdi, H., Mlayah, A., 2021a. Use of lignite as a low-cost material for cadmium and copper removal from aqueous solutions: assessment of adsorption characteristics and exploration of involved mechanisms. Water (Switzerland) 13, 164. https://doi.org/10.3390/w13020164.

Jellali, S., Charabi, Y., Usman, M., Al-Badi, A., Jeguirim, M., 2021b. Investigations on biogas recovery from anaerobic digestion of raw sludge and its mixture with agri-food wastes: application to the largest industrial estate in Oman. Sustain. Times 13, 3698. https://doi.org/10.3390/su13073698.

Jellali, S., Diamantopoulos, E., Haddad, K., Anane, M., Durner, W., Mlayah, A., 2016. Lead removal from aqueous solutions by raw sawdust and magnesium pretreated biochar: experimental investigations and numerical modelling. J. Environ. Manag. 180 https://doi.org/10.1016/j.jenvman.2016.05.055.

Jellali, S., El-Bassi, L., Charabi, Y., Uaman, M., Khiari, B., Al-Wardy, M., Jeguirim, M., 2022b. Recent advancements on biochars enrichment with ammonium and nitrates from wastewaters: a critical review on benefits for environment and agriculture. J. Environ. Manag. 305, 114368 https://doi.org/10.1016/j.jenvman.2021.114368.

Jellali, S., El-Bassi, L., Charabi, Y., Uaman, M., Khiari, B., Al-Wardy, M., Jeguirim, M., 2022c. Recent advancements on biochars enrichment with ammonium and nitrates from wastewaters: a critical review on benefits for environment and agriculture. J. Environ. Manag. 305, 114368 https://doi.org/10.1016/j.jenvman.2021.114368.

Jellali, S., Khiari, B., Usman, M., Hamdi, H., Charabi, Y., Jeguirim, M., 2021c. Sludge-derived biochars: a review on the influence of synthesis conditions on pollutants removal efficiency from wastewaters. Renew. Sustain. Energy Rev. 144, 111068 https://doi.org/10.1016/j.rser.2021.111068.

Jha, S., Nanda, S., Acharya, B., Dalai, A.K., 2022. A review of thermochemical conversion of waste biomass to biofuels. Energies 15, 1–23. https://doi.org/10.3390/en15176352.

Jiang, D., Chu, B., Amano, Y., Machida, M., 2018. Removal and recovery of phosphate from water by Mg-laden biochar: batch and column studies. Colloids Surfaces A Physicochem. Eng. Asp. 558, 429–437. https://doi.org/10.1016/j.colsurfa.2018.09.016.

Jiang, M., Yang, Y., Lei, T., Ye, Z., Huang, S., Fu, X., Liu, P., Li, H., 2022. Removal of phosphate by a novel activated sewage sludge biochar: equilibrium, kinetic and mechanism studies. Appl. Energy Combust. Sci. 9, 100056 https://doi.org/10.1016/j.jaecs.2022.100056.

Kang, J., Parsons, J., Gunukula, S., Tran, D.T., 2022. Iron and magnesium impregnation of avocado seed biochar for aqueous phosphate removal. Cleanroom Technol. 4, 690–702. https://doi.org/10.3390/cleantechnol4030042.

Latawiec, A.E., Królczyk, J.B., Kuboń, M., Szwedziak, K., Drosik, A., Polańczyk, E., Grotkiewicz, K., Strassburg, B.B.N., 2017. Willingness to adopt biochar in agriculture: the producer's perspective. Sustain. Times 9, 1–13. https://doi.org/10.3390/su9040655.

Li, B., Jing, F., Hu, Z., Liu, Y., Xiao, B., Guo, D., 2021. Simultaneous recovery of nitrogen and phosphorus from biogas slurry by Fe-modified biochar. J. Saudi Chem. Soc. 25, 101213 https://doi.org/10.1016/j.jscs.2021.101213.

Li, J., Cao, L., Li, B., Huang, H., Yu, W., Sun, C., Long, K., Young, B., 2023. Utilization of activated sludge and shell wastes for the preparation of Ca-loaded biochar for phosphate removal and recovery. J. Clean. Prod. 382, 135395 https://doi.org/10.1016/j.jclepro.2022.135395.

Li, J., Li, B., Huang, H., Lv, X., Zhao, N., Guo, G., Zhang, D., 2019. Removal of phosphate from aqueous solution by dolomite-modified biochar derived from urban dewatered sewage sludge. Sci. Total Environ. 687, 460–469. https://doi.org/10.1016/j.scitotenv.2019.05.400.

Li, S., Ma, X., Ma, Z., Dong, X., Wei, Z., Liu, X., zhu, L., 2021. Mg/Al-layered double hydroxide modified biochar for simultaneous removal phosphate and nitrate from aqueous solution. Environ. Technol. Innov. 23, 101771 https://doi.org/10.1016/j.eti.2021.101771.

Li, Y., Azeem, M., Luo, Y., Peng, Y., Feng, C., Li, R., Peng, J., Zhang, L., Wang, H., Zhang, Z., 2022. Phosphate capture from biogas slurry with magnesium-doped biochar composite derived from Lycium chinensis branch filings: performance, mechanism, and effect of coexisting ions. Environ. Sci. Pollut. Res. 29, 84873–84885. https://doi.org/10.1007/s11356-022-21625-9.

Liang, J., Ye, J., Shi, C., Zhang, P., Guo, J., Zubair, M., Chang, J., Zhang, L., 2022. Pyrolysis temperature regulates sludge-derived biochar production, phosphate adsorption and phosphate retention in soil. J. Environ. Chem. Eng. 10, 107744 https://doi.org/10.1016/j.jece.2022.107744.

Liang, Q., Fu, X., Wang, P., Li, X., Zheng, P., 2022. Dynamic adsorption characteristics of phosphorus using MBCQ. Water (Switzerland) 14, 508. https://doi.org/10.3390/w14030508.

Liao, Y., Chen, S., Zheng, Q., Huang, B., Zhang, J., Fu, H., Gao, H., 2022. Removal and recovery of phosphorus from solution by bifunctional biochar. Inorg. Chem. Commun. 139, 109341 https://doi.org/10.1016/j.inoche.2022.109341.

Liu, B., Gai, S., Lan, Y., Cheng, K., Yang, F., 2022a. Metal-based adsorbents for water eutrophication remediation: a review of performances and mechanisms. Environ. Res. 212, 113353 https://doi.org/10.1016/j.envres.2022.113353.

Liu, L., Zheng, X., Wei, X., Kai, Z., Xu, Y., 2021. Excessive application of chemical fertilizer and organophosphorus pesticides induced total phosphorus loss from planting causing surface water eutrophication. Sci. Rep. 11, 23015 https://doi.org/10.1038/s41598-021-02521-7.

Liu, M., Li, R., Wang, J., Liu, X., Li, S., Shen, W., 2022b. Recovery of phosphate from aqueous solution by dewatered dry sludge biochar and its feasibility in fertilizer use. Sci. Total Environ. 814, 152752 https://doi.org/10.1016/j.scitotenv.2021.152752.

Liu, X., Fu, J., Tang, Y., Smith, R.L., Qi, X., 2021. Mg-coordinated self-assembly of MgO-doped ordered mesoporous carbons for selective recovery of phosphorus from aqueous solutions. Chem. Eng. J. 406, 126748 https://doi.org/10.1016/j.cej.2020.126748.

Liu, X., Lv, J., 2023. Efficient phosphate removal from wastewater by Ca-laden biochar composites prepared from eggshell and peanut shells: a comparison of methods. Sustainability 15, 1778. https://doi.org/10.3390/su15031778.

Liu, X., Zhou, W., Feng, L., Wu, L., Lv, J., Du, W., 2022c. Characteristics and mechanisms of phosphorous adsorption by peanut shell-derived biochar modified with magnesium chloride by ultrasonic-assisted impregnation. ACS Omega 7, 43102–43110. https://doi.org/10.1021/acsomega.2c05474.

Liu, Y., Jin, J., Li, J., Zou, Z., Lei, R., Sun, J., Xia, J., 2022d. Enhanced phosphorus recovery as vivianite from anaerobically digested sewage sludge with magnetic biochar addition. Sustain. Times 14, 8690. https://doi.org/10.3390/su14148690.

Lu, Z., Zhang, K., Liu, F., Gao, X., Zhai, Z., Li, J., Du, L., 2022. Simultaneous recovery of ammonium and phosphate from aqueous solutions using Mg/Fe modified NaY zeolite: integration between adsorption and struvite precipitation. Sep. Purif. Technol. 299, 121713 https://doi.org/10.1016/j.seppur.2022.121713.

Ludemann, C.I., Gruere, A., Heffer, P., Dobermann, A., 2022. Global data on fertilizer use by crop and by country. Sci. Data 9, 1–8. https://doi.org/10.1038/s41597-022-01592-z.

Luo, D., Wang, L., Nan, H., Cao, Y., Wang, H., Kumar, T.V., Wang, C., 2022. Phosphorus adsorption by functionalized biochar: a review. Environ. Chem. Lett. 21, 497–524. https://doi.org/10.1007/s10311-022-01519-5.

Lv, B., Zhang, W., Xu, D., Li, S., Hu, J., Fan, X., 2022. Influence of different metals on production of sewage sludge–based biochar and its application for ammonium and phosphate adsorption removal from wastewater. J. Environ. Eng. 148, 04022051 https://doi.org/10.1061/(asce)ee.1943-7870.0002039.

Ma, X., Li, S., Ren, H., Zhang, Y., Ma, Z., 2022. Egg white-mediated fabrication of Mg/Al-LDH-Hard biochar composite for phosphate adsorption. Molecules 27, 8951. https://doi.org/10.3390/molecules27248951.

Missau, J., Rodrigues, M.A.S., Bertuol, D.A., Tanabe, E.H., 2022. Phosphate adsorption improvement using a novel adsorbent by CaFe/LDH supported onto CO2 activated biochar. Water Sci. Technol. 86, 2396–2414. https://doi.org/10.2166/wst.2022.332.

Murtaza, G., Ahmed, Z., Eldin, S.M., Ali, B., Bawazeer, S., Usman, M., Iqbal, R., Neupane, D., Ullah, A., Khan, A., Hassan, M.U., Ali, I., Tariq, A., 2023. Biochar-Soil-Plant interactions: a cross talk for sustainable agriculture under changing climate. Front. Environ. Sci. 11 https://doi.org/10.3389/fenvs.2023.1059449.

Nardis, B.O., Franca, J.R., Carneiro, J.S. da S., Soares, J.R., Guilherme, L.R.G., Silva, C.A., Melo, L.C.A., 2022. Production of engineered-biochar under different pyrolysis conditions for phosphorus removal from aqueous solution. Sci. Total Environ. 816, 151559 https://doi.org/10.1016/j.scitotenv.2021.151559.

Nardis, B.O., Santana Da Silva Carneiro, J., Souza, I.M.G. De, Barros, R.G. De, Azevedo Melo, L.C., 2021. Phosphorus recovery using magnesium-enriched biochar and its potential use as fertilizer. Arch. Agron Soil Sci. 67, 1017–1033. https://doi.org/10.1080/03650340.2020.1771699.

Neal, C., Jarvie, H.P., 2005. Agriculture, community, river eutrophication and the water framework directive. Hydrol. Process. 19, 1895–1901. https://doi.org/10.1002/hyp.5903.

Niemmanee, T., Borwornchokchai, K., Nindam, T., 2019. Farmer's perception, knowledge and attitude toward the use of biochar for agricultural soil improvement in Amphawa district, Samut Songkhram province. ACM Int. Conf. Proceeding Ser. 39–43. https://doi.org/10.1145/3323716.3323758.

Oladejo, J., Shi, K., Luo, X., Yang, G., Wu, T., 2019. A review of sludge-to-energy recovery methods. Energies. https://doi.org/10.3390/en12010060.

Pathy, A., Ray, J., Paramasivan, B., 2021. Challenges and opportunities of nutrient recovery from human urine using biochar for fertilizer applications. J. Clean. Prod. 304, 127019 https://doi.org/10.1016/j.jclepro.2021.127019.

Paul, E., Laval, M.L., Sperandio, M., 2001. Excess sludge production and costs due to phosphorus removal. Environ. Technol. 22, 1363–1371. https://doi.org/10.1080/09593332208618195.

Phuong Tran, T.C., Nguyen, T.P., Nguyen, T.T., Le, P.C., Tran, Q.B., Nguyen, X.C., 2022. Equilibrium single and co-adsorption of nutrients from aqueous solution onto aluminium-modified biochar. Case Stud. Chem. Environ. Eng. 5, 100181 https://doi.org/10.1016/j.cscee.2022.100181.

Pourhashem, G., Hung, S.Y., Medlock, K.B., Masiello, C.A., 2019. Policy support for biochar: review and recommendations. GCB Bioenergy 11, 364–380. https://doi.org/10.1111/gcbb.12582.

Priya, E., 2022. Comprehensive review on technological advances of adsorption for removing nitrate and phosphate from waste water. In: Kumar, S., Verma, C., Sarkar, S., Maji, P.K. (Eds.), A Comprehensive Review on Technological Advances of Adsorption for Removing Nitrate and Phosphate from Waste Water. J. Water Process Eng, vol. 49, 103159. https://doi.org/10.1016/j.jwpe.2022.103159.

Qin, J., Zhang, C., Chen, Z., Wang, X., Zhang, Y., Guo, L., 2022. Converting wastes to resource: utilization of dewatered municipal sludge for calcium-based biochar adsorbent preparation and land application as a fertilizer. Chemosphere 298, 134302. https://doi.org/10.1016/j.chemosphere.2022.134302.

Qin, Y., Wu, X., Huang, Q., Beiyuan, J., Wang, J., Liu, J., Yuan, W., Nie, C., Wang, H., 2023. Phosphate removal mechanisms in aqueous solutions by three different Fe-modified biochars. Int. J. Environ. Res. Publ. Health 20, 326. https://doi.org/10.3390/ijerph20010326.

Qu, J., Akindolie, M.S., Feng, Y., Jiang, Z., Zhang, G., Jiang, Q., Deng, F., Cao, B., Zhang, Y., 2020. One-pot hydrothermal synthesis of NaLa(CO3)2 decorated magnetic biochar for efficient phosphate removal from water: kinetics, isotherms, thermodynamics, mechanisms and reusability exploration. Chem. Eng. J. 394, 124915 https://doi.org/10.1016/j.cej.2020.124915.

Rangabhashiyam, S., Balasubramanian, P., 2019. The potential of lignocellulosic biomass precursors for biochar production: performance, mechanism and wastewater application—a review. Ind. Crop. Prod. 128, 405–423. https://doi.org/10.1016/j.indcrop.2018.11.041.

Ren, L., Li, Y., Wang, K., Ding, K., Sha, M., Cao, Y., Kong, F., Wang, S., 2021. Recovery of phosphorus from eutrophic water using nano zero-valent iron-modified biochar and its utilization. Chemosphere 284, 131391. https://doi.org/10.1016/j.chemosphere.2021.131391.

Roberts, K.G., Gloy, B.A., Joseph, S., Scott, N.R., Lehmann, J., 2010. Life cycle assessment of biochar systems: estimating the energetic, economic, and climate change potential. Environ. Sci. Technol. 44, 827–833. https://doi.org/10.1021/es902266r.

Rogers, P.M., Fridahl, M., Yanda, P., Hansson, A., Pauline, N., Haikola, S., 2022. Socio-economic determinants for biochar deployment in the southern highlands of Tanzania. Energies 15, 1–19. https://doi.org/10.3390/en15010144.

Shakoor, M.B., Ye, Z.L., Chen, S., 2021. Engineered biochars for recovering phosphate and ammonium from wastewater: a review. Sci. Total Environ. 779, 146240 https://doi.org/10.1016/j.scitotenv.2021.146240.

Shang, Z., Wang, Y., Wang, S., Jin, F., Hu, Z., 2022. Enhanced phosphorus removal of constructed wetland modified with novel Lanthanum-ammonia-modified hydrothermal biochar: performance and mechanism. Chem. Eng. J. 449, 137818 https://doi.org/10.1016/j.cej.2022.137818.

Shin, H., Tiwari, D., Kim, D.J., 2020. Phosphate adsorption/desorption kinetics and P bioavailability of Mg-biochar from ground coffee waste. J. Water Process Eng. 37, 101484 https://doi.org/10.1016/j.jwpe.2020.101484.

Sun, C., Cao, H., Huang, C., Wang, P., Yin, J., Liu, H., Tian, H., Xu, H., Zhu, J., Liu, Z., 2022. Eggshell based biochar for highly efficient adsorption and recovery of

phosphorus from aqueous solution: kinetics, mechanism and potential as phosphorus fertilizer. Bioresour. Technol. 362, 127851 https://doi.org/10.1016/j.biortech.2022.127851.
Sun, E., Zhang, Y., Xiao, Q., Li, H., Qu, P., Yong, C., Wang, B., Feng, Y., Huang, H., Yang, L., Hunter, C., 2022. Formable porous biochar loaded with La - Fe (hydr) oxides/montmorillonite for efficient removal of phosphorus in wastewater : process and mechanisms. Biochar 4, 1–19. https://doi.org/10.1007/s42773-022-00177-8.
Tao, X., Huang, T., Lv, B., 2020. Synthesis of fe/mg-biochar nanocomposites for phosphate removal. Materials 13. https://doi.org/10.3390/ma13040816.
Tran, D.T., Pham, Thuy Duong, Dang, V.C., Pham, Thanh Dong, Nguyen, M.V., Dang, N. M., Ha, M.N., Nguyen, V.N., Nghiem, L.D., 2022. A facile technique to prepare MgO-biochar nanocomposites for cationic and anionic nutrient removal. J. Water Process Eng. 47, 102702 https://doi.org/10.1016/j.jwpe.2022.102702.
Tripathi, N., Hills, C.D., Singh, R.S., Atkinson, C.J., 2019. Biomass waste utilisation in low-carbon products: harnessing a major potential resource. npj Clim. Atmos. Sci. 2, 35. https://doi.org/10.1038/s41612-019-0093-5.
Tursi, A., 2019. A review on biomass: importance, chemistry, classification, and conversion. Biofuel Res. J. 6, 962–979. https://doi.org/10.18331/BRJ2019.6.2.3.
USEPA, 1995. Ecological Restoration: a Tool to Manage Stream Quality, Report EPA (Washington, DC, US).
van Puijenbroek, P.J.T.M., Beusen, A.H.W., Bouwman, A.F., 2019. Global nitrogen and phosphorus in urban waste water based on the Shared Socio-economic pathways. J. Environ. Manag. 231, 446–456. https://doi.org/10.1016/j.jenvman.2018.10.048.
Van Truong, T., Kim, Y.J., Kim, D.J., 2023. Study of biochar impregnated with Al recovered from water sludge for phosphate adsorption/desorption. J. Clean. Prod. 383, 135507 https://doi.org/10.1016/j.jclepro.2022.135507.
Vijay, V., Shreedhar, S., Adlak, K., Payyanad, S., Sreedharan, V., Gopi, G., Sophia van der Voort, T., Malarvizhi, P., Yi, S., Gebert, J., Aravind, P.V., 2021. Review of large-scale biochar field-trials for soil amendment and the observed influences on crop yield variations. Front. Energy Res. 9, 1–21. https://doi.org/10.3389/fenrg.2021.710766.
Vikrant, K., Kim, K.H., Ok, Y.S., Tsang, D.C.W., Tsang, Y.F., Giri, B.S., Singh, R.S., 2018. Engineered/designer biochar for the removal of phosphate in water and wastewater. Sci. Total Environ. 616–617, 1242–1260. https://doi.org/10.1016/j.scitotenv.2017.10.193.
Wahab, M.A., Hassine, R.B., Jellali, S., 2011. Removal of phosphorus from aqueous solution by Posidonia oceanica fibers using continuous stirring tank reactor. J. Hazard Mater. 189, 577–585. https://doi.org/10.1016/j.jhazmat.2011.02.079.
Wang, C., Luo, D., Zhang, X., Huang, R., Cao, Y., Liu, G., Zhang, Y., Wang, H., 2022. Biochar-based slow-release of fertilizers for sustainable agriculture: a mini review. Environ. Sci. Ecotechnology 10, 100167. https://doi.org/10.1016/j.ese.2022.100167.
Wang, H., Xiao, K., Yang, J., Yu, Z., Yu, W., Xu, Q., Wu, Q., Liang, S., Hu, J., Hou, H., Liu, B., 2020. Phosphorus recovery from the liquid phase of anaerobic digestate using biochar derived from iron−rich sludge: a potential phosphorus fertilizer. Water Res. 174, 115629 https://doi.org/10.1016/j.watres.2020.115629.
Wang, L., Wang, J., Wei, Y., 2021. Facile synthesis of eggshell biochar beads for superior aqueous phosphate adsorption with potential urine P-recovery. Colloids Surfaces A Physicochem. Eng. Asp. 622, 126589 https://doi.org/10.1016/j.colsurfa.2021.126589.
Wang, P., Zhi, M., Cui, G., Chu, Z., Wang, S., 2021. A comparative study on phosphate removal from water using Phragmites australis biochars loaded with different metal oxides. R. Soc. Open Sci. 8, 201789 https://doi.org/10.1098/rsos.201789.
Witek-Krowiak, A., Gorazda, K., Szopa, D., Trzaska, K., Moustakas, K., Chojnacka, K., 2022. Phosphorus recovery from wastewater and bio-based waste: an overview. Bioengineered 13, 13474–13506. https://doi.org/10.1080/21655979.2022.2077894.
Xiang, L., Liu, S., Ye, S., Yang, H., Song, B., Qin, F., Shen, M., Tan, C., Zeng, G., Tan, X., 2021. Potential hazards of biochar: the negative environmental impacts of biochar applications. J. Hazard Mater. 420, 126611 https://doi.org/10.1016/j.jhazmat.2021.126611.
Xu, Y., Liao, H., Zhang, J., Lu, H., He, X., Zhang, Y., Wu, Z., Wang, H., Lu, M., 2022. A novel Ca-modified biochar for efficient recovery of phosphorus from aqueous solution and its application as a phosphorus biofertilizer. Nanomaterials 12, 2755. https://doi.org/10.3390/nano12162755.
Yang, F., Chen, Y., Nan, H., Pei, L., Huang, Y., Cao, X., Xu, X., Zhao, L., 2021. Metal chloride-loaded biochar for phosphorus recovery: noteworthy roles of inherent minerals in precursor. Chemosphere 266, 128991. https://doi.org/10.1016/j.chemosphere.2020.128991.
Yang, J., Zhang, M., Wang, H., Xue, J., Lv, Q., Pang, G., 2021. Efficient recovery of phosphate from aqueous solution using biochar derived from co-pyrolysis of sewage sludge with eggshell. J. Environ. Chem. Eng. 9, 105354 https://doi.org/10.1016/j.jece.2021.105354.
Yang, L., Liang, C., Shen, F., Hu, M., Zhu, W., Dai, L., 2023. A critical review on the development of lanthanum-engineered biochar for environmental applications. J. Environ. Manag. 332, 117318 https://doi.org/10.1016/j.jenvman.2023.117318.
Yang, Y., Kou, L., Fan, Q., Jiang, K., Wang, J., 2022. Simultaneous recovery of phosphate and degradation of antibiotics by waste sludge-derived biochar. Chemosphere 291, 132832. https://doi.org/10.1016/j.chemosphere.2021.132832.
Yilmaz, S., Selim, H., 2013. A review on the methods for biomass to energy conversion systems design. Renew. Sustain. Energy Rev. 25, 420–430. https://doi.org/10.1016/j.rser.2013.05.015.
Yin, H., Zhang, M., Huo, L., Yang, P., 2022. Efficient removal of phosphorus from constructed wetlands using solidified lanthanum/aluminum amended attapulgite/biochar composite as a novel phosphorus filter. Sci. Total Environ. 833, 155233 https://doi.org/10.1016/j.scitotenv.2022.155233.
Yuan, J., Wen, Y., Ruiz, G., Sun, W., Ma, X., 2020. Enhanced phosphorus removal and recovery by metallic nanoparticles-modified biochar. Nanotechnol. Environ. Eng. 5 https://doi.org/10.1007/s41204-020-00090-0.
Zeng, S., Kan, E., 2022. Sustainable use of Ca(OH)2 modified biochar for phosphorus recovery and tetracycline removal from water. Sci. Total Environ. 839, 156159 https://doi.org/10.1016/j.scitotenv.2022.156159.
Zhang, C., Dong, Y., Liu, W., Yang, D., Liu, J., Lu, Y., Lin, H., 2023. Enhanced adsorption of phosphate from pickling wastewater by Fe-N co-pyrolysis biochar: performance, mechanism and reusability. Bioresour. Technol. 369, 128263 https://doi.org/10.1016/j.biortech.2022.128263.
Zhang, J., Huang, W., Yang, D., Xiang, J., Chen, Y., 2022. Removal and recovery of phosphorus from secondary effluent using layered double hydroxide-biochar composites. Sci. Total Environ. 844, 156802 https://doi.org/10.1016/j.scitotenv.2022.156802.
Zhang, M., Chen, Q., Zhang, R., Zhang, Y., Wang, F., He, M., Guo, X., Yang, J., Zhang, X., Mu, J., 2023. Pyrolysis of Ca/Fe-rich antibiotic fermentation residues into biochars for efficient phosphate removal/recovery from wastewater: turning hazardous waste to phosphorous fertilizer. Sci. Total Environ. 869, 161732 https://doi.org/10.1016/j.scitotenv.2023.161732.
Zhang, M., Yang, J., Wang, H., Lv, Q., Xue, J., 2021a. Enhanced removal of phosphate from aqueous solution using Mg/Fe modified biochar derived from excess activated sludge: removal mechanism and environmental risk. Environ. Sci. Pollut. Res. 28, 16282–16297. https://doi.org/10.1007/s11356-020-12180-2.
Zhang, P., Duan, W., Peng, H., Pan, B., Xing, B., 2022a. Functional biochar and its balanced design. ACS Environ. Au 2, 115–127. https://doi.org/10.1021/acsenvironau.1c00032.
Zhang, P., He, M., Huo, S., Li, F., Li, K., 2022b. Recent progress in metal-based composites toward adsorptive removal of phosphate: mechanisms, behaviors, and prospects. Chem. Eng. J. 446, 137081 https://doi.org/10.1016/j.cej.2022.137081.
Zhang, Y., Akindolie, M.S., Tian, X., Wu, B., Hu, Q., Jiang, Z., Wang, L., Tao, Y., Cao, B., Qu, J., 2021b. Enhanced phosphate scavenging with effective recovery by magnetic porous biochar supported La(OH)3: kinetics, isotherms, mechanisms and applications for water and real wastewater. Bioresour. Technol. 319 https://doi.org/10.1016/j.biortech.2020.124232.
Zhang, Y., Shi, G., Wu, W., Ali, A., Wang, H., Wang, Q., Xu, Z., Qi, W., Li, R., Zhang, Z., 2022c. Magnetic biochar composite decorated with amino-containing biopolymer for phosphorus recovery from swine wastewater. Colloids Surfaces A Physicochem. Eng. Asp. 634, 127980 https://doi.org/10.1016/j.colsurfa.2021.127980.
Zhang, Z., Yu, H., Zhu, R., Zhang, X., Yan, L., 2020. Phosphate adsorption performance and mechanisms by nanoporous biochar–iron oxides from aqueous solutions. Environ. Sci. Pollut. Res. 27, 28132–28145. https://doi.org/10.1007/s11356-020-09166-5.
Zhao, D., Luo, Y., Feng, Y. yang, He, Q. ping, Zhang, L. sheng, Zhang, K.qiang, Wang, F., 2021. Enhanced adsorption of phosphorus in soil by lanthanum-modified biochar: improving phosphorus retention and storage capacity. Environ. Sci. Pollut. Res. 28, 68982–68995. https://doi.org/10.1007/s11356-021-15364-6.
Zhao, Y., Yang, H., Xia, S., Wu, Z., 2022. Removal of ammonia nitrogen, nitrate, and phosphate from aqueous solution using biochar derived from Thalia dealbata Fraser: effect of carbonization temperature. Environ. Sci. Pollut. Res. 29, 57773–57789. https://doi.org/10.1007/s11356-022-19870-z.
Zhao, Z., Wang, B., Zhang, X., Xu, H., Cheng, N., Feng, Q., Zhao, R., Gao, Y., Wei, M., 2022. Release characteristics of phosphate from ball-milled biochar and its potential effects on plant growth. Sci. Total Environ. 821, 153256 https://doi.org/10.1016/j.scitotenv.2022.153256.
Zheng, Q., Yang, L., Song, D., Zhang, S., Wu, H., Li, S., Wang, X., 2020. High adsorption capacity of Mg–Al-modified biochar for phosphate and its potential for phosphate interception in soil. Chemosphere 259, 127469. https://doi.org/10.1016/j.chemosphere.2020.127469.
Zheng, Y., Zimmerman, A.R., Gao, B., 2020. Comparative investigation of characteristics and phosphate removal by engineered biochars with different loadings of magnesium, aluminum, or iron. Sci. Total Environ. 747, 141277 https://doi.org/10.1016/j.scitotenv.2020.141277.
Zhou, C., Wang, Y., 2020. Recent progress in the conversion of biomass wastes into functional materials for value-added applications. Sci. Technol. Adv. Mater. 21, 787–804. https://doi.org/10.1080/14686996.2020.1848213.
Zhu, D., Chen, Y., Yang, H., Wang, S., Wang, X., Zhang, S., Chen, H., 2020. Synthesis and characterization of magnesium oxide nanoparticle-containing biochar composites for efficient phosphorus removal from aqueous solution. Chemosphere 247, 125847. https://doi.org/10.1016/j.chemosphere.2020.125847.
Zhuo, S.N., Dai, T.C., Ren, H.Y., Liu, B.F., 2022. Simultaneous adsorption of phosphate and tetracycline by calcium modified corn stover biochar: performance and mechanism. Bioresour. Technol. 359, 127477 https://doi.org/10.1016/j.biortech.2022.127477.